Chapter 6 METEOROLOGY AND HYDROLOGY

Chapter 6

METEOROLOGY AND HYDROLOGY

Contents

List of Figures

List of Tables

Chapter 6 METEOROLOGY AND HYDROLOGY

6.1 Outlines of Meteorology and Hydrology

6.1.1 General

The Köprübaşi project site is located on the midstream stretch of the Devrek River, a tributary of the Filyos River, which runs through the northwest part of Turkey. The Filyos River rises from Mt. Köroğlu (EL. 2,378m) approximately 100 km northwest of Ankara, changing its name from Gerede River to Soğanlı River to Yenice River in order from the upstream. The Yenice River merges with the tributary Devrek River approximately 30 km upstream from its mouth to become the Filyos River and empties into the Black Sea. The length of the Filyos River is approximately 350 km, the catchment area is approximately 13,300 km^2 and the annual average runoff at Derecikviran (Gauging Station No.1335) near the river mouth is 104.6 m^3/s.

The Devrek River on which the project site is to be located rises from Lake Abant situated approximately 30 km southwest of Bolu. The stream, after leaving Lake Abant, becomes the Büyüksu River, merges with the Mengen River in the vicinity of Gökçesu, and changes its name to the Devrek River.

The Devrek River is the largest tributary of the Filyos River. Its total length is approximately 150 km, the catchment area approximately 3,130 km^2, and the annual average runoff 22.9 m^3/s in the vicinity of Devrek (Gauging Station No.13-44 approximately 20 km upstream from the confluence).

The northern part of the Filyos River basin is subject to the influence of the Black Sea climate in which there generally is much rain and it is temperate. Precipitation decreases going from north to south, differences in air temperature between winter and summer increase, and the southern part of the basin is influenced by the continental climate of Central Anatolia.

This may be comprehended from the fact that whereas the annual average precipitation is 1,220 mm and the annual mean temperature 13.5°C at Zonguldak facing the Black Sea, at Çerkes in the southeast part of the basin, they are 386 mm and 7.8°C respectively.

Annual average precipitations in the Devrek River basin are 775 mm at Devrek, 537 mm at Bolu, and 640 mm at Pazarköy. Annual mean temperatures are 13.5°C at Devrek, 10.2°C at Bolu, and 9.5°C at Pazarköy. There is snowfall in the wintertime in the basin, the annual average numbers of days of snowfall being 8.3 days at Devrek, 25.3 days at Bolu, and 27.4 days at Pazarköy.

6.1.2 Meteorological and Hydrological Observation Data

The meteorological stations and gauging stations shown in Figure 6-1 exist in the basin and surrounding area of the Project. Of these, meteorological stations are owned by DMI and observations are being carried out. On the other hand, gauging stations are owned by DSI or EIE who are carrying out observations. The observation periods of the principal meteorological stations are given in Table 6-1 and those of the principal gauging stations in Table 6-2.

Of the meteorological stations in the river basin, Yeniçağa station and Gökçesu station nearest to the project site were closed down in recent years.

6.1.3 Meteorology and Hydrology of Project Area

The four meteorological stations of Bolu, Yeniçağa, Pazarköy, and Gökçesu are located within the river basin of the Project as shown in Figure 6-1. Annual average precipitations in the basin are from 500 to 680 mm, the quantity being seen to increase as one goes further downstream. Most of the precipitation occurs from November to June, with the monthly amounts during this

period being approximately 50 to 60 mm, the rainfall occurring in the rainy season being equalized. There is not much precipitation from July to September. The monthly average precipitations at the meteorological stations listed in Table 6-1 are given in Table 6-3.

The Bolu and Pazarköy meteorological stations are where continuous observations are being carried out on air temperatures and humidities within the river basin of the Project. The monthly mean air temperatures and average humidities in the basin and its surroundings are given in Tables 6-4 and 6-5.

Monthly maximum wind speeds and wind directions are given in Table 6-6, numbers of average monthly days of snowfall in Table 6-7, and highest snow depth by month in Table 6-8.

Meanwhile, the runoff in the project area is roughly 6.5 to 8 $\ell/s/km^2$ (0.65 to 0.8 m^3/s per 100 km^2), the monthly runoffs being large from February to May, and minimum from August to October. The ratio of minimum to maximum monthly average runoff is approximately 1:8.

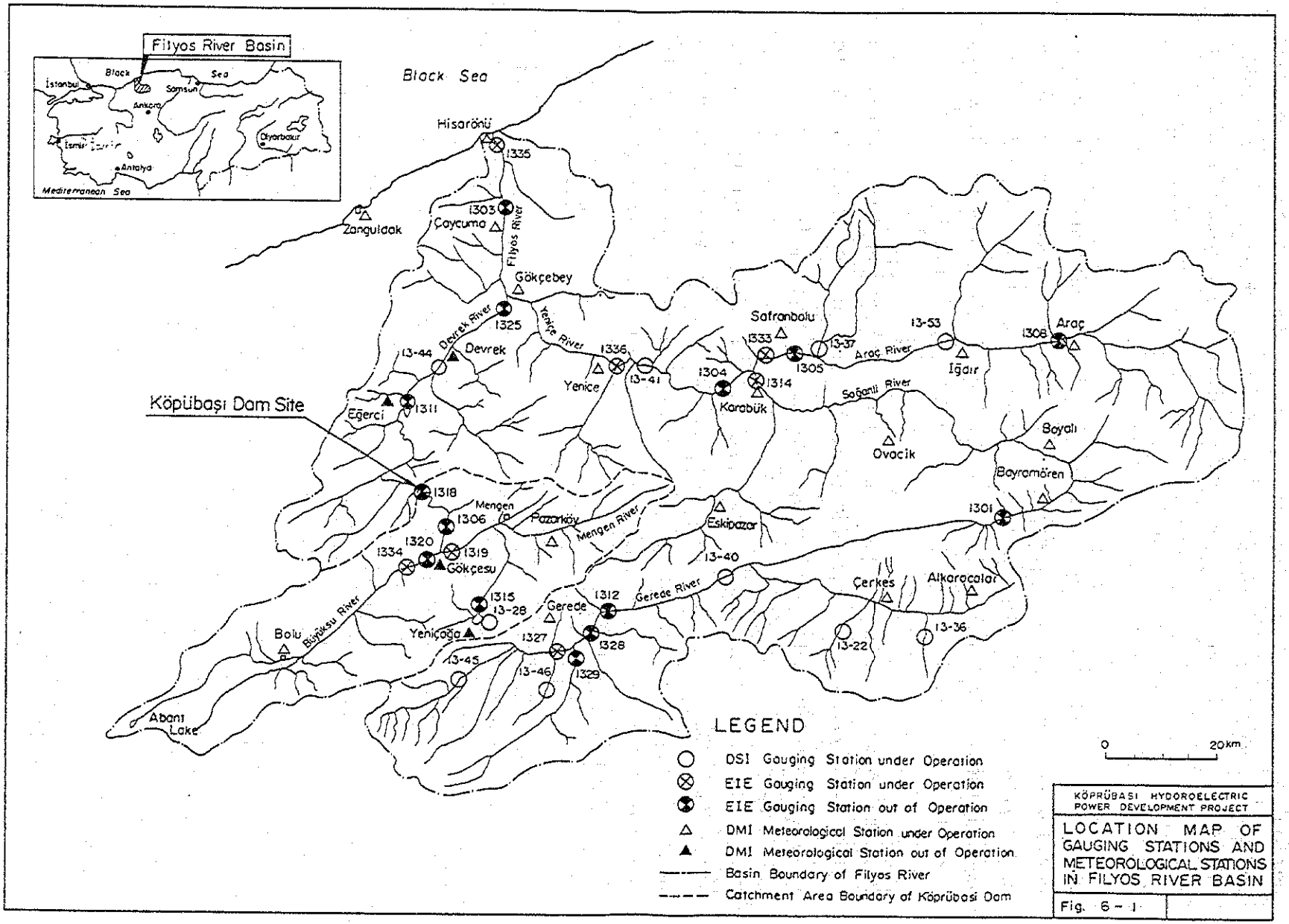
Filyos River Basin
Black Sea
İstanbul
Samsun
Ankara
İzmir
Antalya
Diyarbakır
Mediterranean Sea
Black Sea
Hisarönü
1335
Zonguldak
1303
Çaycuma
Filyos River
Gökçebey
1325
Devrek River
Devrek
13-44
Yenice River
1336
Yenice
13-41
Köpübaşı Dam Site
Eğerci
1311
1318
Mengen
1306
Pazarköy
Mengen River
1320
1334
1319
Gökçesu
1315
13-28
Gerede
1312
Gerede River
Yeniçoğa
1327
1328
1329
13-45
13-46
Bolu
Büyüksu River
Abant Lake
Safranbolu
1333
1305
13-37
Araç River
13-53
Araç
1308
Iğdır
1304
1314
Karabük
Soğanlı River
Ovacik
Boyalı
Bayramören
1301
Eskipazar
13-40
Çerkes
Alkaracalar
13-22
13-36
LEGEND
DSI Gauging Station under Operation
EIE Gauging Station under Operation
EIE Gauging Station out of Operation
DMI Meteorological Station under Operation
DMI Meteorological Station out of Operation
Basin Boundary of Filyos River
Catchment Area Boundary of Köpübaşı Dam
0
20km
KÖPRÜBAŞI HYDROELECTRIC POWER DEVELOPMENT PROJECT
LOCATION MAP OF GAUGING STATIONS AND METEOROLOGICAL STATIONS IN FILYOS RIVER BASIN
Fig. 6 - 1

Table 6-1 List of Meteorological Stations in the Project Area and Vicinity

Station	Elevation (m)	Observation Period (Year)								
			1930	40	50	60	70	80	90	
Bolu	742	1929								
Yeniçaga	950					1964				Closed in 1992
Pazarköy	740			1943						
Gökçesu	500					1965				Closed in 1991
Gerede	1,270				1957					
Devrek	100		1950							Closed in 1992 for Removement
Zonguldak	130		1931							

Table 6-2 List of Gauging Stations in the Project Area and Vicinity

Station No.	Station Name	River	Catchment Area (km²)	Observation Period (Water Year)	Remarks
1306	Gökçesu (EIE)	Devrek	1,895.6	1954 – 62	Out of operation
1311	Gürdere (EIE)	Devrek	2,420.0	1958 – 71	Out of operation
1318	Köprübaşı (EIE)	Devrek	1,944.0	1965 – 71	Out of operation
1319	Gökçesu (Mengen, EIE)	Mengen	766.4	1965 – 89	
1320	Bolu (EIE)	Büyüksu	1,102.8	1965 – 66	Out of operation
1334	Beşdeğirmenler (EIE)	Büyüksu	1,102.0	1967 – 89	
13-44	Devrek (DSI)	Devrek	2,640.0	1983 – 91	

Table 6-3 Monthly Average Precipitation in and around the Project Area

Unit: mm

Station	Period	Jan.	Feb.	Mar.	Apr.	May	June	July	Aug.	Sep.	Oct.	Nov.	Dec.	Total
Bolu	1929-90	58.5	47.8	48.1	48.7	58.4	52.0	26.5	20.4	28.8	37.1	49.1	61.7	537.1
Yeniçağa	1964-87	46.2	36.4	44.0	49.0	69.7	56.7	27.5	27.9	26.1	34.5	40.0	53.6	511.4
Pazarköy	1943-90	62.2	52.3	57.0	65.4	78.0	66.3	32.8	26.8	34.9	49.3	53.1	62.2	640.3
Gökçesu	1965-90	71.1	47.5	52.8	62.1	74.4	59.9	35.1	43.0	30.1	57.0	64.8	85.7	683.5
Gerede	1957-90	64.7	51.2	58.0	65.8	87.5	71.4	35.9	25.3	34.9	39.0	52.0	72.6	658.3
Devrek	1950-91	80.0	63.6	57.6	53.0	63.5	60.5	48.0	49.6	52.2	75.1	84.8	87.1	775.0
Zonguldak	1931-90	141.3	102.5	92.1	69.2	53.8	69.9	72.8	86.5	95.2	144.7	146.4	145.7	1220.1

Table 6-4 Monthly Mean Temperature in and around the Project Area

Unit: °C

Station	Period	Jan.	Feb.	Mar.	Apr.	May	June	July	Aug.	Sep.	Oct.	Nov.	Dec.	Average
Bolu	1929-90	0.4	1.6	4.5	9.5	13.8	17.0	19.4	19.5	15.7	11.5	6.9	2.7	10.2
Pazarköy	1965-91	0.3	1.7	4.6	9.1	13.0	16.2	18.4	18.1	14.7	10.5	5.9	2.1	9.5
Gerede	1963-86	-2.5	-1.0	2.3	6.9	11.0	14.3	16.7	16.5	13.3	9.1	4.5	-0.1	7.6
Devrek	1965-90	4.7	5.6	7.6	12.6	16.6	20.1	22.5	22.2	18.8	14.0	10.1	6.5	13.5
Zonguldak	1937-90	6.0	6.2	7.2	11.0	15.2	19.4	21.6	21.4	18.4	14.9	11.7	8.5	13.5

Table 6-5 Monthly Average Humidity in and around the Project Area

Unit: %

Station	Period	Jan.	Feb.	Mar.	Apr.	May	June	July	Aug.	Sep.	Oct.	Nov.	Dec.	Average
Bolu	1930-90	77	75	72	69	72	71	68	67	70	74	76	78	72
Pazarköy	1964-90	80	77	74	70	73	72	72	71	75	78	79	81	75
Gerede	1964-90	77	73	69	61	62	64	61	61	62	63	68	76	66
Devrek	1964-90	72	71	67	63	65	64	64	65	66	68	69	72	67
Zonguldak	1937-90	70	70	71	72	74	73	73	73	73	74	70	69	72

Table 6-6 Monthly Maximum Wind Velocity and Direction in and around the Project Area

Unit: m/s

Station	Period	Jan.	Feb.	Mar.	Apr.	May	June	July	Aug.	Sep.	Oct.	Nov.	Dec.	Max.
Bolu	1937-90	24.5	23.6	28.5	26.9	21.6	21.0	20.9	28.9	18.1	20.5	24.0	23.5	28.9
		S	S	SW	SSE	S	W	W	W	W	W	WSW	NW	W
Zonguldak	1937-90	36.4	31.8	29.5	31.5	27.8	28.2	23.8	31.5	28.4	25.2	32.0	29.2	36.4
		N	SSE	SSW	SW	W	SSE	WSW	WNW	NW	NNE	SSE	SSW	N

Table 6-7 Number of Snowing Days in and around the Project Area

Unit: day

Station	Period	Jan.	Feb.	Mar.	Apr.	May	June	July	Aug.	Sep.	Oct.	Nov.	Dec.	Total
Bolu	1956-90	7.5	7.2	4.5	0.5	-	-	-	-	-	0.1	1.3	4.3	25.4
Yeniçağa	1964-88	6.6	6.0	4.4	1.5	0.0	-	-	-	-	0.1	1.7	4.6	24.9
Pazarköy	1956-90	8.0	7.7	4.9	0.7	-	-	-	-	-	-	1.5	4.6	27.4
Gökçesu	1965-89	5.8	4.8	3.2	-	-	-	-	-	-	-	1.3	2.8	17.9
Gerede	1957-90	12.4	11.0	8.1	3.3	0.2	-	-	-	-	0.7	2.4	8.6	46.7
Devrek	1950-90	3.4	2.8	1.0	-	-	-	-	-	-	-	0.3	0.9	8.4

Table 6-8 Highest Snow Depth in and around the Projectd Area

Unit: cm

Station	Period	Jan.	Feb.	Mar.	Apr.	May	June	July	Aug.	Sep.	Oct.	Nov.	Dec.	Max.
Bolu	1929-90	66	72	57	13	-	-	-	-	-	-	53	66	72
Yeniçağa	1964-90	65	50	45	22	2	-	-	-	-	6	35	65	65
Pazarköy	1943-90	72	88	87	15	7	-	-	-	-	6	87	73	88
Gökçesu	1965-89	50	54	40	7	-	-	-	-	-	1	44	57	57
Gerede	1957-90	90	120	148	22	2	-	-	-	-	16	60	76	148
Devrek	1950-90	55	83	55	-	-	-	-	-	-	-	20	27	83
Zanguldak	1936-85	105	96	61	-	-	-	-	-	-	-	25	17	105

6.2 Runoff at Project Site

6.2.1 Representative Gauging Stations

Gauging Station No.1318 was installed at the Köprübaşi damsite (Master Plan damsite) in 1964, but was abolished in 1972. In calculation of runoff at the project site, the data of this gauging station was used for the period from the 1965 water year (October 1964 to September 1965) to the 1971 water year for which there were runoff records. Runoff observations of the No. 1319 and No.1334 gauging stations are being continued. Accordingly, runoff data of the two gauging stations located respectively on the Büyüksu River and the Mengen River, two main tributaries upstream of the damsite, can be used for calculation of runoff after 1972 water year.

6.2.2 Catchment Area of Damsite

Because of the reason described in Chapter 9, the following are adopted for catchment area of each damsite respectively, and used for calculation of runoff at the sites.

Damsite	Catchment Area (km^2)
Master Plan Damsite	1,994
Upstream Damsite	1,959

6.2.3 Supplementation of Runoff Data

Supplementation of runoff data was done regarding monthly runoffs (unit: MCM).

The correlation between runoff of No.1318 Gauging Station and summation of runoffs of No.1319 and No.1334 stations was obtained to supplement runoff data after No.1318 had been closed down. In the water years of 1967 to 1971 when the observation periods

of the three gauging stations overlapped, the following is obtained (see Figure 6-2).

$$Y = 1.0401 * X + 0.5720$$

Correlation coefficient (hereafter referred to as R) = 0.997

where, X = Summation of runoffs of No.1319 and No.1334 stations

Y = Runoff at No.1318 station

Next, for supplementation of runoff data for the period before installation of Gauging Station No.1318, the correlation below was calculated. When the period was taken to be the 1965 to 1971 water years, the following was obtained (see Figure 6-3).

$$Y = 0.7962X - 0.3793$$

$$R = 0.991$$

where, X = Runoff at No.1311 station

Y = Runoff at No.1318 station

Similarly, when the period was taken to be the 1958 to 1962 water years, the result is as below (see Figure 6-4).

$$Y = 1.2652X - 3.0440$$

$$R = 0.974$$

where, X = Runoff at No.1306 station

Y = Runoff at No.1311 station

And regarding the supplementation after water year 1990 for which the runoff data of the No.1319 and No.1334 gauging stations had not yet been arranged, when a period of the water years from 1983 to 1990 were taken, the results were as follows (see Figure 6-5):

$$Y = 0.5052X - 3.4867$$

$$R = 0.938$$

where, X = Runoff at No. 13-44 station

Y = Summation of runoffs of No.1319 and No.1334 stations

Based on the results above, correlations for the runoff data of the these gauging stations were recognized to exist.

6.2.4 Verification of Runoff Data

Firstly, as shown in Table 6-9, a period in which runoff observations were being made at a plural number of gauging stations was selected, and specific discharge (runoff per square kilometer) was calculated for each station. Extreme differences could not be recognized between periods and it is considered there was no error which existed over the entire observation period.

Next, double mass curves were prepared using runoffs of individual gauging stations and precipitations at meteorological stations near guaging stations. The combinations of gauging stations and meteorological stations are shown below.

Gauging Station	Meteorological Observatory	Period (Water Year)
No. 1318	Bolu & Pazarköy	1965-1971
No. 1319	Pazarköy	1965-1988
No. 1334	Bolu	1967-1989
No. 13-44	Devrek	1986-1991
No. 1311	Bolu & Pazarköy	1958-1971
No. 1306	Bolu & Pazarköy	1954-1962

The double mass curves mentioned above are shown in Figures 6-6 through 6-11.

Among these, a part of the double mass curve for Gauging Station No. 1306 shows a sudden change in gradient (corresponding to water year 1956). On the other hand, no abnormality can be seen for this period from the double mass curves for the sum of the precipitations at the Bolu and Pazarköy meteorological stations and the precipitation of Zonguldak meteorological station

(period: 1954-1962 water years, see Figure 6-12). Therefore, the runoff data for the water years 1954-1955 were discarded.

Otherwise, these are no sudden changes in double mass curves for runoff and precipitation and the runoff data are considered to be reasonable.

6.2.5 Runoff at Damsite

Based on the above study, the natural inflows at the Master Plan and upstream damsites were obtained calculating the runoff at Gauging Station No.1318 by relational expressions and ratios of catchment areas of gauging stations as shown in Table 6-10. The results are shown in Tables 6-11 and 6-12. The natural inflow at the Master Plan damsite is thus an annual average of 14.4 m^3/s, with specific discharge of 7.2 $\ell/s/km^2$ (0.72 m^3/s per 100 km^2).

The spectral analysis results of precipitations at the Bolu and Pazarköy meteorological stations are shown in Figure 6-13 and the spectral analysis result of the natural inflow at the Master Plan damsite in Figure 6-14.

Precipitation at Bolu meteorological station has periodicities of approximately 12 and 4 years and that at Pazarköy approximately 10 years and 4 years. The natural inflow at the damsite has periodicities of approximately 12 years and 4 years. In general, it is said that analyses on periodicities have accuracies at those of less than about 1/5 of the calculation period. The calculation period of the natural inflow at the damsite is 36 years, and the periodicity of approximately 12 years would lack reliability with only analysis of natural inflow, but since the two meteorological stations upstream of the dam have periodicities of 10 to 12 years, it may be considered that natural inflow also has periodicity of this degree.

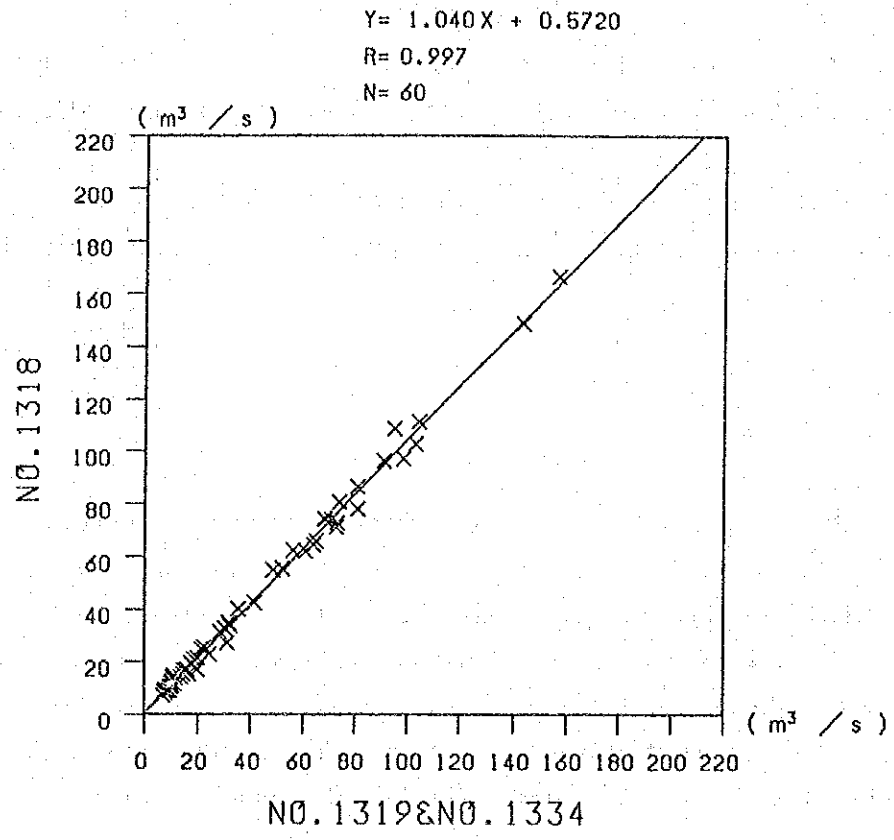

Figure 6-2 **Correlation between Sum of Runoffs at No.1319 & No.1334 G.S.s and Runoff at No.1318 G.S.**

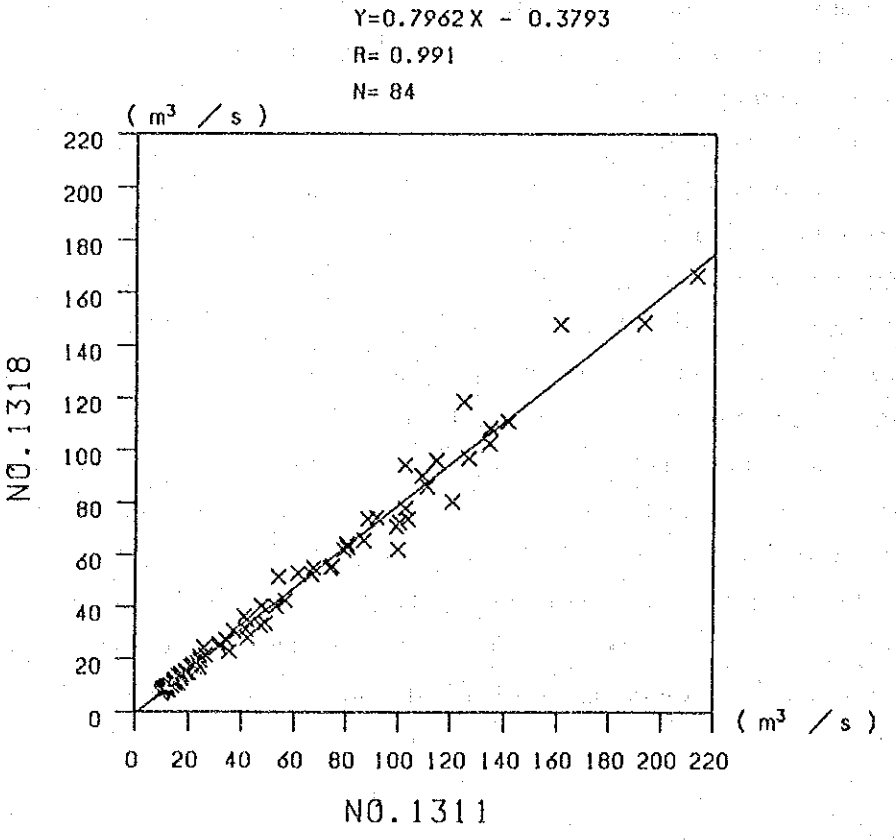

Figure 6-3 **Correlation between Runoff at No.1311 G.S. and Runoff at No.1318 G.S.**

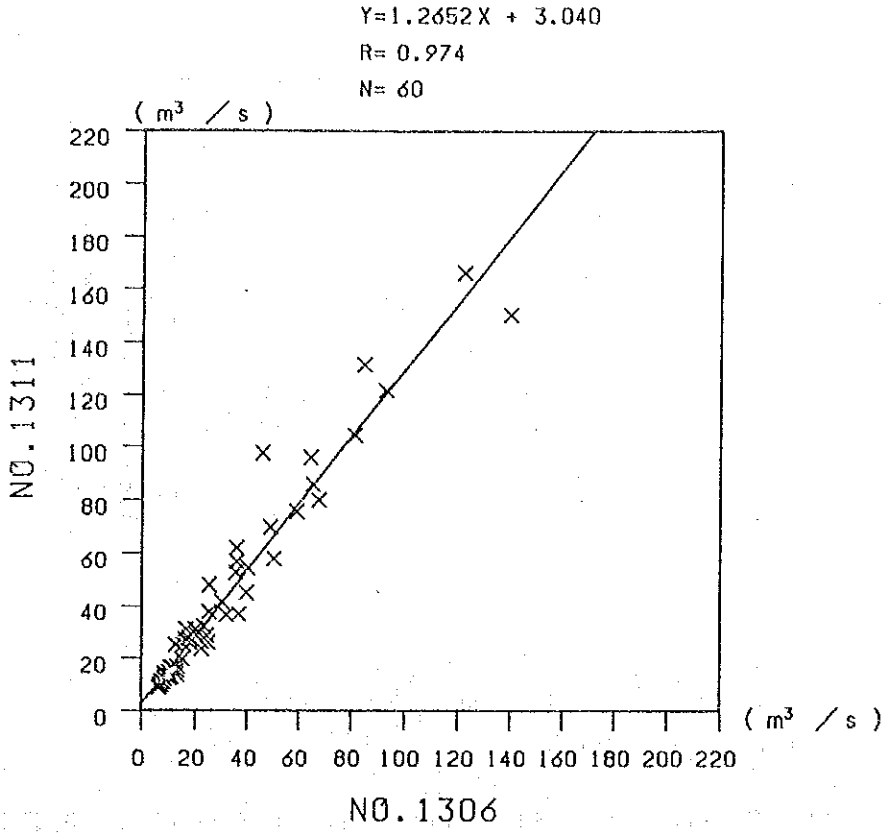

Figure 6-4 **Correlation between Runoff at No.1306 G.S. and Runoff at No.1311 G.S.**

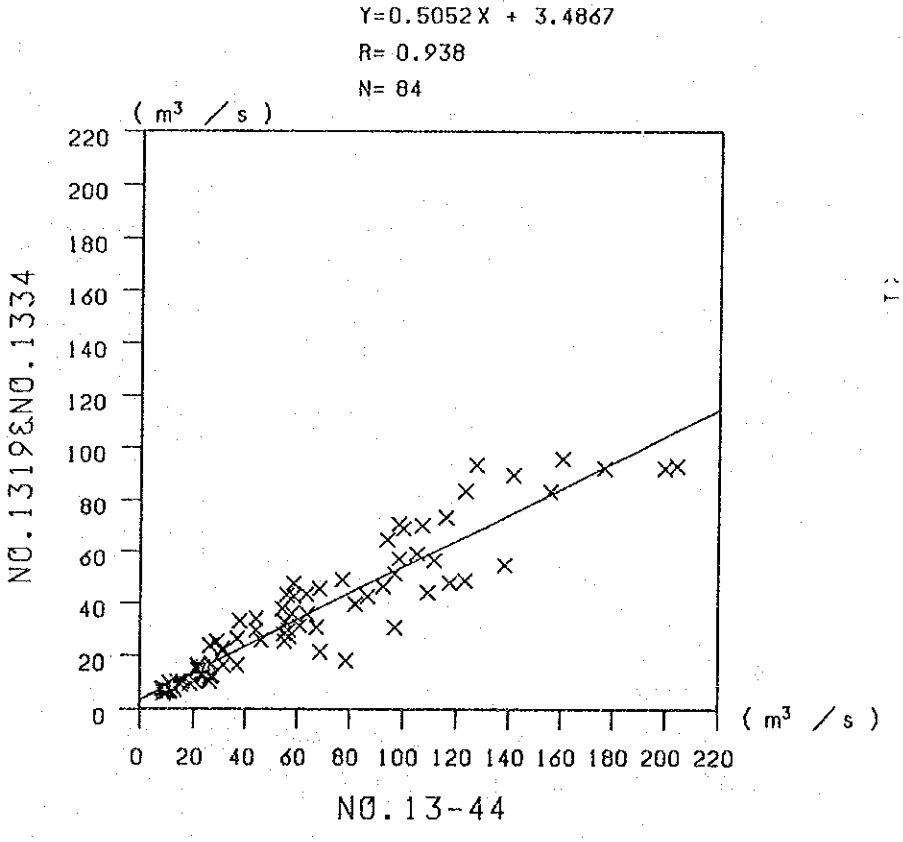

Figure 6-5 **Correlation between Runoff at No.13-44 G.S. and Sum of Runoffs at No.1319 & No.1334 G.S.s**

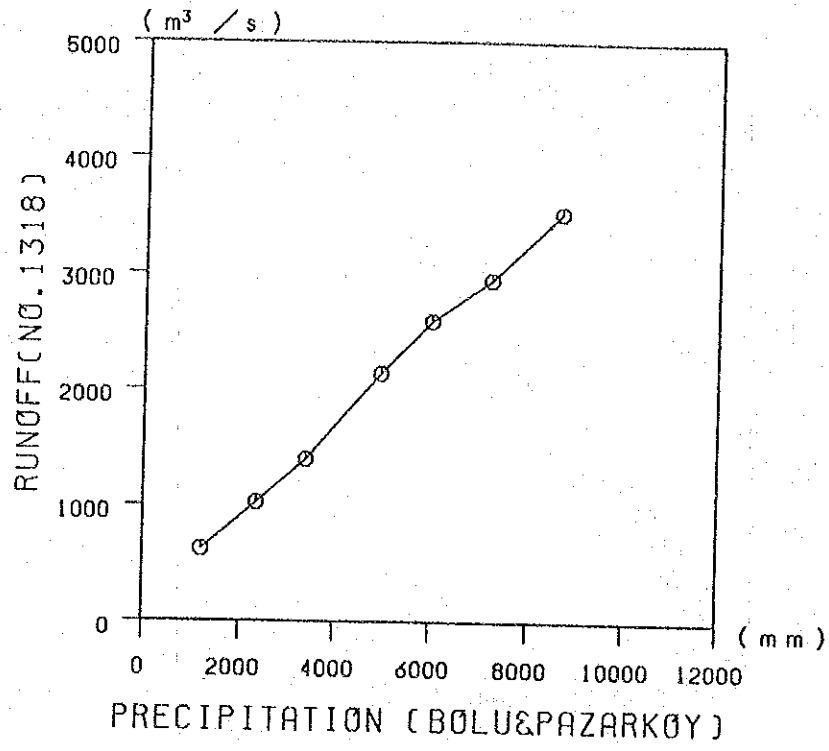

Figure 6-6 **Double Mass Curve of Sum of Precipitations at Bolu & Pazarköy M.S.s and Runoff at No.1318 G.S.**

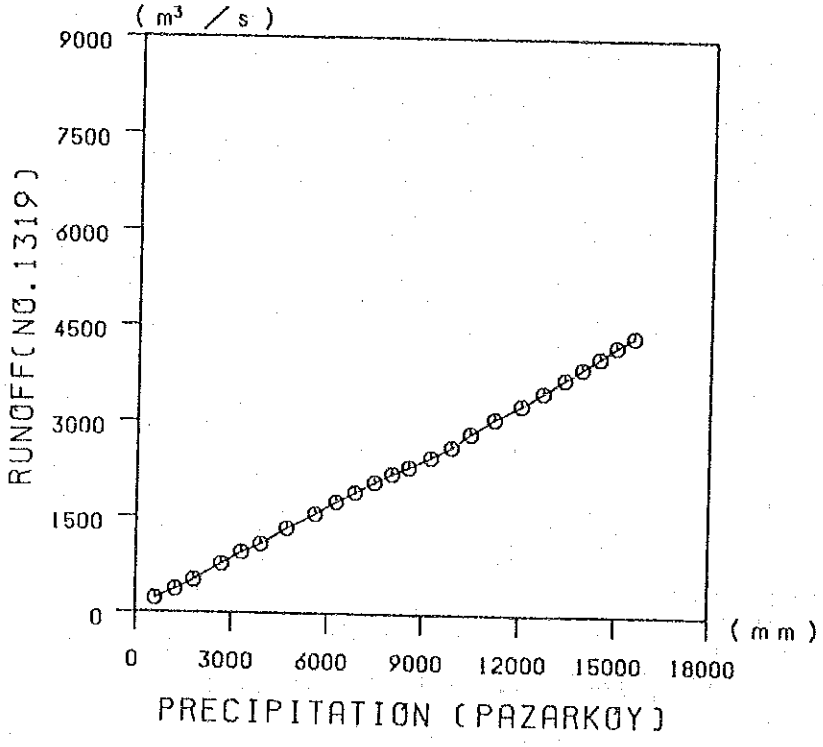

Figure 6-7 **Double Mass Curve of Precipitation at Pazarköy M.S. and Runoff at No.1319 G.S.**

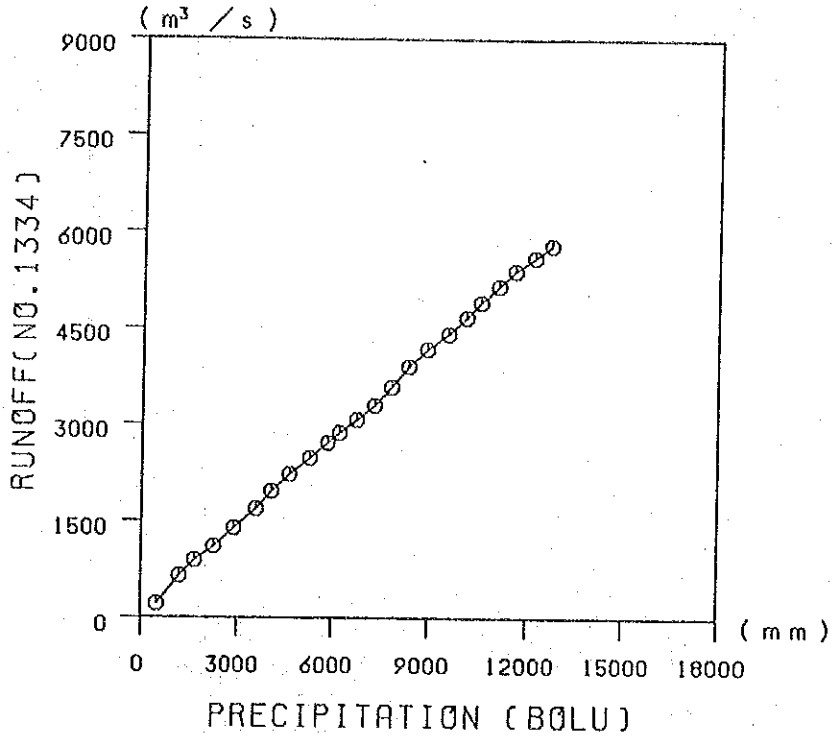

Figure 6-8 **Double Mass Curve of Precipitation at Bolu M.S. and Runoff at No.1334 G.S.**

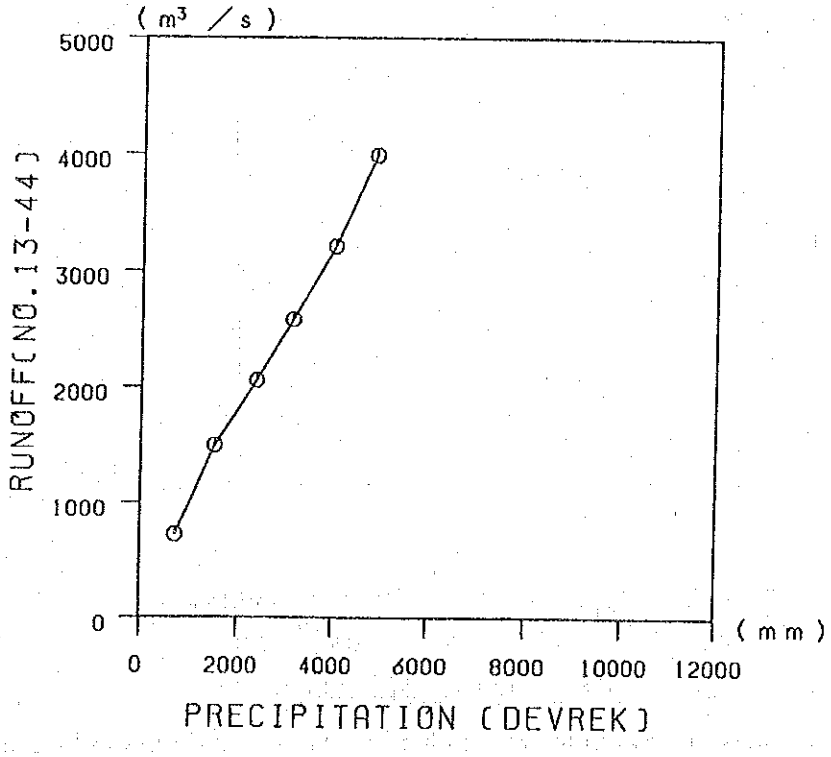

Figure 6-9 **Double Mass Curve of Precipitation at Devrek M.S. and Runoff at No.13-44 G.S.**

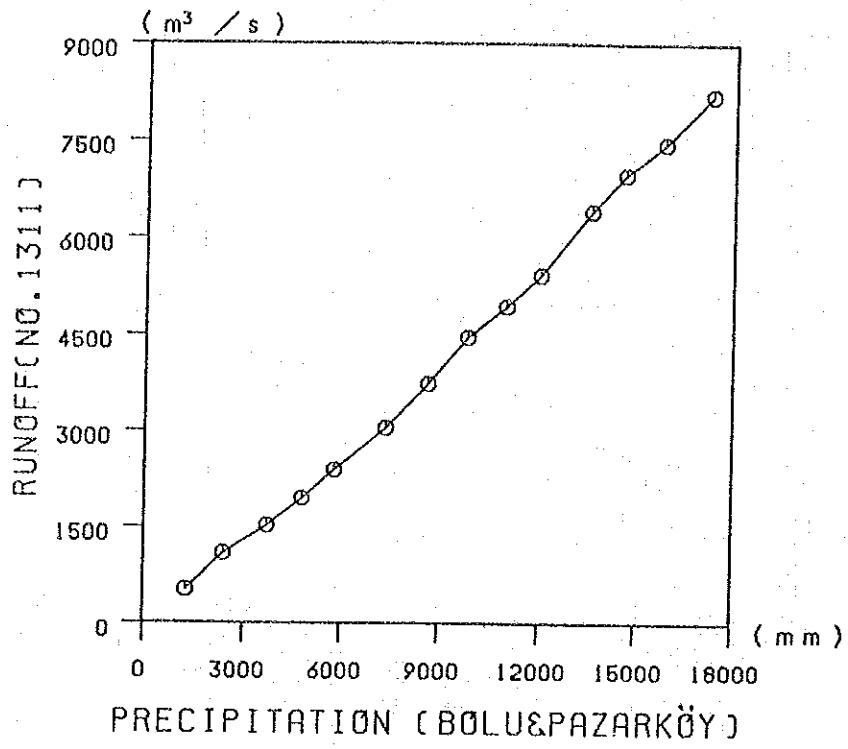

Figure 6-10 Double Mass Curve of Sum of Precipitations at Bolu & Pazarköy M.Ss and Runoff at No. 1311 G.S.

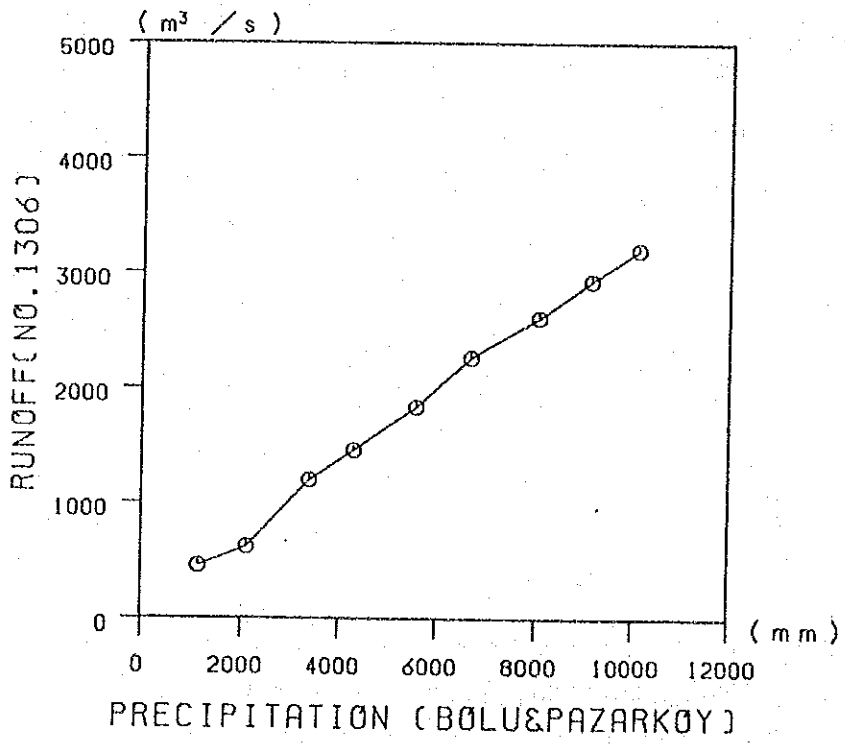

Figure 6-11 Double Mass Curve of Sum of Precipitations at Bolu & Pazarköy M.Ss and Runoff at No. 1306 G.S.

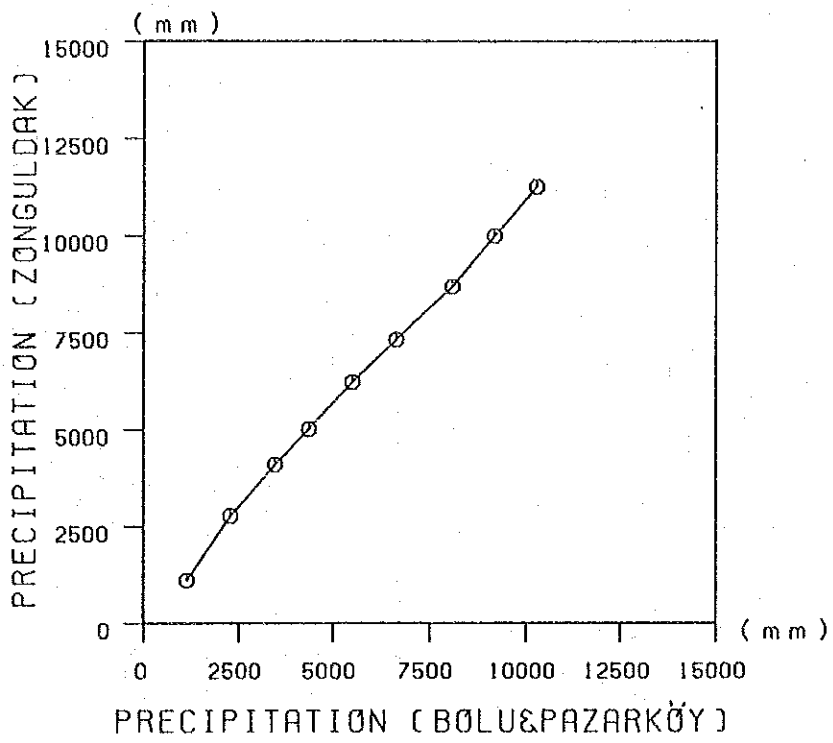

Figure 6-12 **Double Mass Curve of Sum of Precipitations at Bolu & Pazarköy M.Ss and precipitation at Zonguldak M.S.**

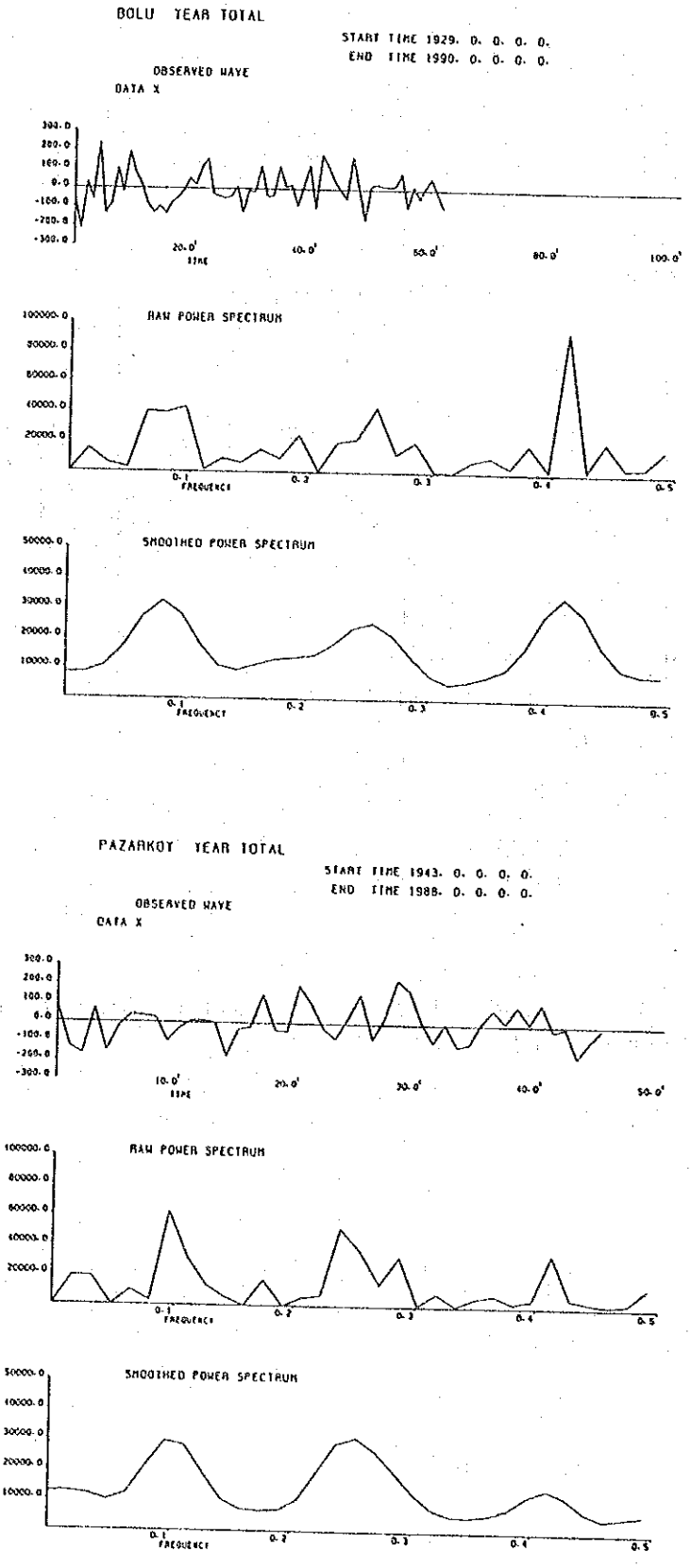

Figure 6-13 Spectral Analysis on Precipitation at Bolu M.S.and Pazarköy M.S.

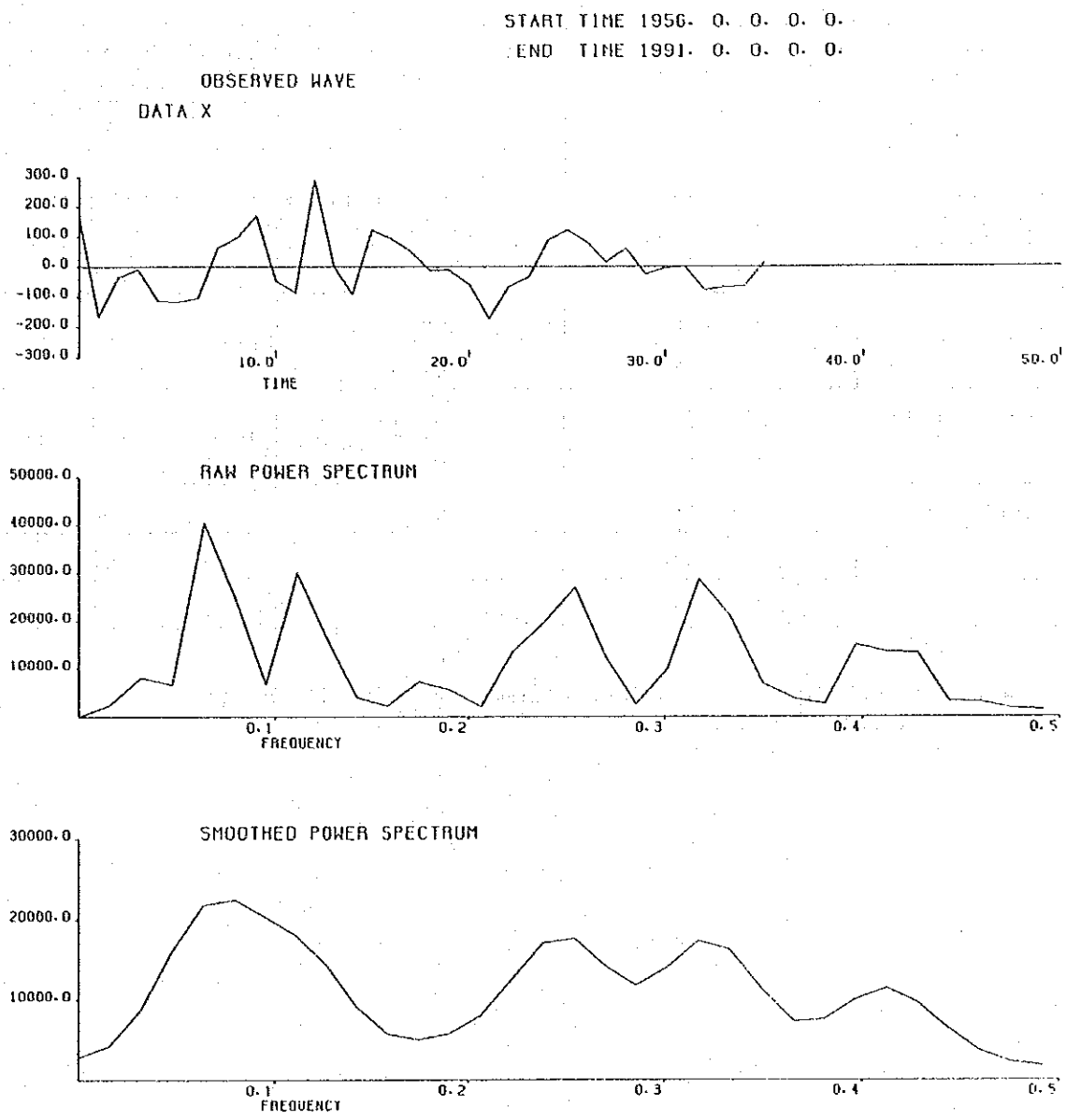

Figure 6-14 Spectral Analysis on Natural Inflow at Master Plan Damsite

Table 6-9 Comparison of Specific Discharge

Period (Water Year)	No. of Station	Catchment Area (km^2)	Specific Discharge ($\ell/s/km^2$)
1958-1962	No.1306	1,895.6	5.86
	No.1311	2,420.0	6.28
1965-1971	No.1311	2,420.0	8.37
	No.1318	1,994.0	8.01
	No.1319	766.4	7.90
	No.1334	1,102.0	(8.05)
1967-1989	No.1319	766.4	7.52
	No.1334	1,102.0	7.25
1983-1989	No.1319	766.4	7.40
	No.1334	1,102.0	6.65
	No.1344	2,640.0	8.75

Note: Figure in the parenthesis shows specific discharge in the period 1967-1971.

Table 6-10 Relational Expressions for Estimation on Runoff at Project Site

Calculation by JICA			Calculation in Master Plan Report		
Period (Water Year)	Applied Station	Relational Expression (Unit: MCM)	Period (Water Year)	Applied Station	Relational Expression (Unit: MCM)
1956-1957	No.1306 & No.1311	Y(No.1311) = 1.2652 * X(No.1306) + 3.0440 Y(No.1318) = 0.7962 * X(No.1311) - 0.3793			
1958-1964	No.1311	Y(No.1318) = 0.7962 * X(No.1311) - 0.3793	1963-1964	No.1311	$Y(No.1318) = 0.7623 * X(No.1311)^{1.0072}$
1965-1971	No.1318		1965-1971	No.1318	
1972-1989	No.1319 & No.1334	Y(No.1318) = X(No.1319 + No.1334) * A(No.1318)/[A(No.1319) + A(No.1334)] where, A(No.1318) = 1,994.0 km^2 A(No.1319) = 766.4 km^2 A(No.1334) = 1,102.0 km^2	1972-1983	No.1319 & No.1334	Y(No.1318) = 1.0410 * X(No.1319 + No.1334) + 0.5177
1990-1991	No.1319, No.1334 & No.13-44	Y(No.1319 + No.1334) = 0.5052 * X(No.13-44) + 3.4867 Y(No.1318) = X(No.1319 + No.1334) * A(No.1318)/[A(No.1319) + A(No.1334)]			
Runoff at Damsites Master Plan Damsite Upstream Damsite where,		Q_{MD} = Y(No.1318) Q_{UD} = A_{UD}/A_{MD} * Y(No.1318) A_{UD} = 1,959.0 km^2 A_{MD} = A(No.1318) = 1,994.0 km^2	Runoff at Damsite		Q_{Dam} = Y(No.1318) * A_{Dam}/A (No.1318) where, A_{Dam} = 2,034.37 km^2 A(No.1318) = 1994.0 km^2

Table 6-11 Monthly Natural Inflow at Master Plan Damsite

Period: 1956-91 C.A.= 1994 km^2
Unit:MCM

Year	Oct.	Nov.	Dec.	Jan.	Feb.	Mar.	Apr.	May	June	July	Aug.	Sept.	Total
1956	18.41	27.04	48.07	66.16	97.72	104.70	121.16	64.19	31.23	12.95	8.09	9.13	608.84
1957	10.57	17.09	19.48	22.43	48.31	50.21	27.41	44.82	21.86	7.83	6.21	8.89	285.12
1958	7.76	8.73	20.44	24.39	41.57	82.73	96.42	42.96	48.97	22.49	10.68	10.63	417.76
1959	10.89	11.32	12.81	21.52	19.79	131.95	119.34	45.82	32.78	19.86	9.52	8.51	444.11
1960	10.29	11.81	10.81	25.45	55.15	59.98	63.36	35.65	29.06	15.33	12.77	9.36	339.03
1961	10.10	9.54	18.53	20.49	44.76	76.17	68.13	28.84	20.77	24.33	7.49	7.58	336.72
1962	7.61	12.62	22.52	21.78	37.82	104.41	77.48	29.64	13.18	7.83	6.72	6.76	348.39
1963	9.85	8.85	33.01	59.98	67.38	79.25	62.02	89.06	58.66	21.97	11.23	12.37	513.52
1964	15.88	17.01	54.60	25.70	68.89	127.10	71.82	69.49	51.80	20.50	11.99	15.09	549.87
1965	13.75	18.60	55.11	40.44	52.29	118.81	148.26	94.56	30.79	28.36	10.77	9.53	621.27
1966	10.12	14.87	34.96	53.12	36.30	62.82	90.45	51.55	24.56	9.96	8.43	9.05	406.19
1967	9.49	8.26	12.25	17.17	16.94	74.00	97.19	71.04	31.47	13.84	7.36	8.65	367.66
1968	10.69	12.80	62.24	80.65	111.17	166.48	148.87	64.29	35.03	15.36	14.21	20.95	742.74
1969	17.74	15.33	25.68	32.75	54.95	74.45	96.32	74.09	27.46	17.13	9.04	9.08	454.02
1970	9.10	11.50	19.44	21.47	55.51	65.75	72.80	42.48	33.72	11.15	8.44	8.35	359.71
1971	9.75	10.71	22.93	62.03	40.08	86.56	108.67	102.74	77.99	24.97	14.93	13.84	575.20
1972	13.51	13.67	38.15	40.38	46.07	91.72	82.46	57.51	67.31	46.27	25.15	22.56	544.79
1973	45.94	46.30	31.08	32.34	63.51	83.85	73.82	48.35	35.34	21.84	13.39	8.84	504.58
1974	12.33	26.74	42.17	19.79	46.53	65.53	58.85	89.17	35.05	17.77	14.63	13.32	441.86
1975	11.09	11.64	17.55	19.01	29.64	66.85	51.10	141.62	41.91	20.07	18.04	11.44	439.95
1976	14.52	14.44	51.86	32.44	39.54	64.67	78.79	37.36	27.55	10.69	11.36	10.53	393.76
1977	11.97	11.46	28.21	20.11	28.79	59.69	47.17	30.10	18.67	9.00	6.14	6.68	277.98
1978	8.70	10.79	11.69	30.02	65.77	53.13	89.99	54.16	17.85	23.37	10.47	9.74	385.68
1979	11.66	12.07	22.65	61.06	74.93	37.78	42.84	43.62	62.67	27.61	11.14	10.13	418.15
1980	13.54	18.68	40.53	50.87	48.61	110.14	112.81	81.87	31.88	11.01	10.52	9.73	540.20
1981	12.67	23.01	58.73	66.14	59.29	136.75	69.39	73.54	31.69	22.80	10.42	10.01	574.43
1982	11.25	16.88	55.32	77.49	38.00	82.88	100.14	55.46	41.21	18.39	20.65	15.93	533.61
1983	13.51	13.00	13.41	23.16	58.38	99.27	89.06	40.44	33.59	38.14	30.06	14.32	466.34
1984	19.49	47.05	49.48	42.17	45.29	60.83	98.43	74.83	31.55	17.33	15.90	10.48	512.83
1985	10.00	17.67	18.10	27.49	51.82	98.46	95.62	50.60	26.98	13.47	8.46	8.11	426.79
1986	12.75	13.23	32.90	88.84	78.25	75.37	45.22	48.35	28.26	10.20	7.43	7.03	447.83
1987	7.88	11.27	17.56	51.03	54.63	60.37	102.11	73.47	38.64	17.87	10.03	7.27	452.13
1988	10.77	16.76	32.96	31.68	27.79	53.06	68.83	36.33	45.03	24.19	8.39	7.07	373.84
1989	11.21	34.88	46.41	29.04	52.22	99.86	35.41	25.35	23.30	11.27	7.36	6.55	382.86
1990	14.70	32.68	57.53	29.90	29.30	41.42	55.01	67.92	22.20	14.60	10.13	9.69	385.08
1991	14.54	19.54	23.13	22.34	55.04	63.44	45.09	41.39	79.29	65.32	19.45	17.57	466.14
Average	12.89	17.44	32.29	38.63	51.17	82.79	80.88	58.96	36.40	19.86	11.86	10.69	453.86

Daily Ave. Runoff 14.392 m^3/s
Specific Discharge 7.218 l/s/km^2

Table 6-12 Monthly Natural Inflow at Upstream Damsite

Period: 1956-91 C.A.= 1959 km^2
Unit:MCM

Year	Oct.	Nov.	Dec.	Jan.	Feb.	Mar.	Apr.	May	June	July	Aug.	Sept.	Total
1956	18.09	26.56	47.23	65.00	96.01	102.86	119.03	63.06	30.68	12.73	7.95	8.97	598.16
1957	10.38	16.79	19.14	22.04	47.46	49.33	26.93	14.03	21.47	7.69	6.11	8.74	280.11
1958	7.62	8.58	20.08	23.96	40.84	81.27	94.73	42.20	48.11	22.09	10.49	10.45	410.42
1959	10.70	11.13	12.58	21.15	19.44	129.63	117.25	45.02	32.21	19.51	9.35	8.36	436.32
1960	10.11	11.60	10.63	25.00	54.19	58.93	62.25	35.02	28.55	15.06	12.55	9.19	333.08
1961	9.92	9.37	18.20	20.13	43.97	74.84	66.94	28.33	20.40	23.90	7.36	7.45	330.81
1962	7.48	12.40	22.12	21.40	37.16	102.58	76.12	29.12	12.95	7.69	6.60	6.64	342.27
1963	9.68	8.69	32.43	58.93	66.20	77.86	60.93	37.50	57.63	21.58	11.03	12.15	504.61
1964	15.60	16.71	53.65	25.25	67.68	124.87	70.56	68.27	50.89	20.14	11.78	14.83	540.22
1965	13.51	18.27	54.14	39.73	51.37	116.72	145.66	92.90	30.25	27.86	10.58	9.36	610.37
1966	9.94	14.61	34.35	52.19	35.66	61.72	88.86	50.65	24.13	9.79	8.28	8.89	399.06
1967	9.32	8.12	12.03	16.87	16.64	72.70	95.48	69.79	30.92	13.60	7.23	8.50	361.21
1968	10.50	12.58	61.15	79.23	109.22	163.56	146.26	63.16	34.42	15.09	13.96	20.58	729.70
1969	17.42	15.06	25.23	32.18	53.99	73.14	94.63	72.79	26.98	16.83	8.88	8.92	446.05
1970	8.94	11.30	19.10	21.09	54.54	64.60	71.52	41.73	33.13	10.95	8.29	8.20	353.40
1971	9.58	10.52	22.53	60.94	39.38	85.04	106.76	100.94	76.62	24.53	14.67	13.60	565.10
1972	13.27	13.43	37.48	39.67	45.26	90.11	81.02	56.50	66.13	45.46	24.71	22.17	535.22
1973	45.14	45.48	30.53	31.77	62.40	82.38	72.52	47.50	34.72	21.45	13.16	8.68	495.73
1974	12.11	26.28	41.43	19.44	45.71	64.38	57.81	87.60	34.43	17.46	14.37	13.09	434.11
1975	10.89	11.44	17.24	18.67	29.12	65.68	50.20	139.13	41.17	19.72	17.72	11.24	432.23
1976	14.27	14.19	50.95	31.87	38.85	63.54	77.41	36.71	27.06	10.51	11.16	10.35	386.85
1977	11.76	11.26	27.71	19.75	28.29	58.64	46.34	29.57	18.34	8.84	6.03	6.56	273.10
1978	8.55	10.60	11.48	29.49	64.62	52.19	88.41	53.21	17.54	22.96	10.29	9.57	378.91
1979	11.46	11.86	22.25	59.98	73.61	37.12	42.09	42.85	61.57	27.12	10.95	9.95	410.81
1980	13.31	18.35	39.82	49.98	47.76	108.20	110.83	80.43	31.32	10.82	10.34	9.56	330.71
1981	12.45	22.61	57.70	64.97	58.25	134.35	68.17	72.25	31.13	22.40	10.23	9.83	564.35
1982	11.05	16.59	54.35	76.13	37.34	81.43	98.38	54.49	40.48	18.07	20.29	15.65	524.25
1983	13.27	12.77	13.18	22.75	57.35	97.53	87.50	39.73	33.00	37.47	29.54	14.07	458.16
1984	19.15	46.23	48.61	41.43	44.50	59.76	96.70	73.52	30.99	17.03	15.62	10.30	503.83
1985	9.82	17.36	17.78	27.01	50.91	96.73	93.94	49.71	26.51	13.23	8.31	7.97	419.30
1986	12.53	13.00	32.32	87.28	76.88	74.04	44.42	47.50	27.76	10.02	7.30	6.91	439.97
1987	7.74	11.07	17.25	50.14	53.67	59.31	100.32	72.18	37.97	17.55	9.86	7.14	444.19
1988	10.58	16.46	32.38	31.12	27.30	61.96	67.62	35.69	45.22	23.77	8.24	6.94	367.28
1989	11.01	34.26	45.60	28.53	51.30	98.11	34.79	24.90	22.89	11.07	7.23	6.44	376.14
1990	14.44	32.11	56.52	29.38	28.79	40.69	54.05	66.73	21.81	14.34	9.96	9.52	378.32
1991	14.28	19.20	22.73	21.95	54.07	62.33	44.30	40.66	77.90	64.17	19.11	17.26	457.95
Average	12.66	17.13	31.72	37.96	50.27	81.34	79.46	57.93	35.76	19.51	11.65	10.50	445.90

Daily Ave. Runoff 14.139 m^3/s
Specific Discharge 7.091 l/s/km^2

6.3 Evaporation

6.3.1 Data Used for Calculation of Evaporation

Evaporation is being measured at Bolu meteorological station (EL. 742 m) within the basin of the project site and evaporation from the reservoir surface was calculated using these observation data. The observed monthly evaporation amounts at Bolu meteorological station are given in Table 6-13.

6.3.2 Calculation Formula for Evaporation

In general, there is a close correlation between evaporation and air temperature, and in case observation data on evaporation in project area cannot be directly used, evaporation is normally calculated using the correlation with air temperature. Hence, the regression equation for air temperature and evaporation at Bolu meteorological station was calculated. The results were as follows (see Figure 6-15):

$$Y = 9.5724 * X - 25.3270$$

$$R = 0.885$$

where, X = Monthly mean air temperature (°C)

Y = Monthly evaporation (mm)

Period: 1961-1990

Evaporation from the reservoir is calculated from air temperature using this equation.

6.3.3 Air Temperature

Relation between elevation and air temperature was used for estimate on air temperature at damsite. Becuse it is generally used in Turkey assumption that difference in elevation of 100 m causes difference in air temperature of 0.5°C, this relation was adopted for estimate on air temperature on reservoir surface

(EL.437 m) by using air temperature at Bolu meteorological station (see Table 6-14).

$$T_{(Reser)} = T_{(Bolu)} + (742-437) \times 0.5/100$$
$$= T_{(Bolu)} + 1.5$$

where, $T_{(Reser)}$: Monthly mean air temperature (°C) on reservoir surface

$T_{(Bolu)}$: Monthly mean air temperature at Bolu meteorological station

Table 6-15 shows monthly air temperatures on reservoir surface based on monthly air temperatures at Bolu meteorological station.

6.3.4 Evaporation from Reservoir Surface

The annual evaporation from the reservoir surface can be computed from the air temperatures in Table 6-15 and the correlation equation for air temperature and evaporation calculated in 6.3.2. Class-A-pan is used for observation of evaporation so that the evaporation obtained by the correlation equation was multiplied by a correction factor of 0.7 to determine evaporation from the reservoir surface. As a result, the annual evaporation was 717 mm (see Table 6-16).

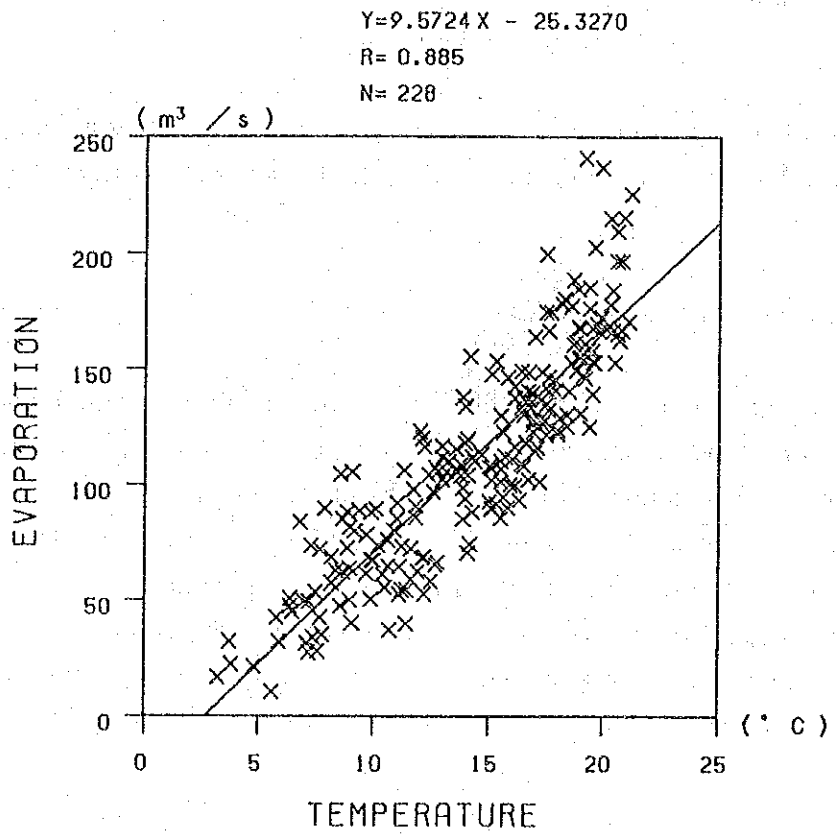

Figure 6-15 Correlation between Temperature and Evaporation at Bolu M.S.

Table 6-13 Monthly Total Evaporation at Bolu Meteorological Station

Unit: mm

Year	Jan.	Feb.	March	Apr.	May	June	July	Aug.	Sept.	Oct.	Nov.	Dec.	Annual
1961	-	-	-	-	-	136.9	176.3	202.7	119.6	64.1	31.3	-	730.9
1962	-	-	-	88.1	147.9	174.7	215.3	225.6	149.1	57.8	39.6	-	1098.1
1963	-	-	-	89.8	105.4	199.9	237.3	215.8	128.0	62.3	33.6	-	1072.1
1964	-	-	-	104.6	116.5	128.1	241.2	174.7	89.4	72.1	-	-	926.6
1965	-	-	-	57.2	108.7	180.7	184.9	178.2	133.7	68.6	-	-	912.0
1966	-	-	-	92.0	116.6	148.5	166.7	178.0	101.2	70.5	36.9	17.0	927.4
1967	-	-	-	88.5	105.5	146.6	167.8	158.2	122.6	68.2	21.5	-	878.9
1968	-	-	-	106.1	142.5	130.7	185.6	130.3	85.2	60.8	42.2	32.0	915.4
1969	-	-	-	83.8	153.4	188.7	166.6	196.7	140.7	73.5	49.3	32.0	1084.7
1970	22.5	-	-	120.0	96.8	137.2	209.6	168.0	107.3	67.1	35.1	-	963.6
1971	-	-	-	63.5	104.3	137.3	161.1	155.2	93.4	81.3	49.4	-	845.5
1972	-	-	-	104.1	155.5	132.4	166.5	139.2	111.2	73.2	47.2	-	929.3
1973	-	-	-	105.4	138.0	137.7	169.4	122.2	118.3	85.5	-	-	876.5
1974	-	-	50.7	71.9	110.1	140.7	161.8	140.6	89.9	92.5	44.9	-	903.1
1975	-	-	-	90.7	85.0	129.1	152.8	125.0	89.9	52.4	42.5	-	767.4
1976	-	-	-	78.2	111.7	112.2	149.6	114.5	87.9	66	28.2	-	748.3
1977	-	-	-	79.6	118.2	126.2	158.4	160.7	106.7	47.2	39.9	-	836.9
1978	-	-	-	62.0	134.1	164.0	154.0	126.2	101.7	58.5	-	-	800.5
1979	-	-	-	72.5	98.6	140.8	145.2	146.2	99.5	54.2	27.3	-	784.3
1980	-	-	-	62.6	112.0	146.5	184.2	152.8	94.1	65.1	-	-	817.3
1981	-	-	-	85.1	97.8	152.8	153.0	147.6	108.1	74.2	-	-	818.6
1982	-	-	-	67.0	102.2	149.0	127.8	125.4	101.2	54.3	-	-	726.9
1983	-	-	-	85.0	110.1	116.4	130.9	128.0	100.0	50.3	10.5	-	731.2
1984	-	-	-	53.2	107.9	109.1	123.6	102.1	121.6	68.6	-	-	686.1
1985	-	-	-	89.3	110.1	131.6	134.9	165.5	113.2	50.1	-	-	794.7
1986	-	-	-	123.0	80.0	123.0	167.7	170.7	116.0	64.5	-	-	844.9
1987	-	-	-	73.5	106.0	128.4	196.9	177.2	132.7	75.8	-	-	890.5
1988	-	-	-	87.9	103.7	117.9	166.7	172.3	130.0	50.2	-	-	828.7
1989	-	-	-	-	115.5	133.3	154.8	162.3	94.5	55.2	-	-	715.6
1990	-	-	-	61.1	107.4	139.9	167.6	154.7	91.5	52.5	-	-	774.7
1991	-	-	-	63.8	90.5	195.1	148.5	132.6	73.7	57.7	-	-	761.9
Average	0.7		1.6	77.7	109.4	143.1	168.6	156.4	108.1	64.3	18.7	2.6	851.4

Table 6-14 Monthly Mean Temperature at Bolu Meteorological Station

Unit:° C

Year	Jan.	Feb.	March	Apr.	May	June	July	Aug.	Sept.	Oct.	Nov.	Dec.	Average
1956	2.4	1.0	0.7	10.5	12.1	17.0	19.1	20.8	13.8	9.9	3.2	-2.5	9.0
1957	-2.2	3.3	4.1	9.8	12.9	18.1	20.9	21.3	18.2	13.3	7.2	2.4	10.8
1958	1.4	5.7	5.6	8.9	15.8	17.2	18.9	19.8	14.6	11.0	6.0	4.2	10.8
1959	2.3	-6.1	1.7	9.2	13.1	16.2	19.8	19.1	12.9	8.6	6.2	5.6	9.1
1960	1.2	1.0	4.2	9.0	15.0	16.4	18.9	18.4	15.6	13.5	8.9	6.2	10.7
1961	-0.7	1.1	4.0	11.7	14.2	17.3	19.4	19.6	14.1	11.1	7.1	3.4	10.2
1962	2.6	1.5	7.6	8.9	15.1	17.5	20.3	21.2	16.4	12.5	11.4	4.5	11.6
1963	1.4	5.7	3.2	7.9	12.8	17.5	19.9	20.9	16.9	11.9	7.4	3.1	10.7
1964	0.0	-1.1	5.1	8.6	12.2	17.2	19.2	17.7	15.1	11.6	6.2	4.5	9.7
1965	1.5	-0.9	5.4	8.2	13.8	18.3	18.9	18.2	16.4	8.2	7.3	5.7	10.1
1966	2.9	6.4	5.5	11.0	13.0	16.7	20.8	20.3	15.5	14.1	10.7	3.2	11.7
1967	-0.8	-2.2	3.2	9.4	13.2	15.8	19.0	19.5	15.6	12.1	4.8	3.6	9.4
1968	-0.6	0.1	3.4	11.3	16.1	16.5	19.4	18.4	15.5	10.4	7.7	3.7	10.2
1969	0.0	2.5	4.3	6.8	15.3	18.7	17.6	20.6	16.7	10.2	7.2	5.9	10.5
1970	3.8	4.8	7.3	12.1	12.6	16.7	20.6	18.9	15.1	10.0	7.8	-0.3	10.8
1971	5.4	2.2	6.1	9.0	14.1	16.5	19.2	19.0	16.3	9.0	7.0	0.1	10.3
1972	-4.5	-0.3	4.1	12.4	14.2	17.6	19.8	19.5	16.0	11.2	6.4	-0.5	9.7
1973	-1.9	4.8	3.7	9.1	13.9	16.1	19.7	18.0	16.6	11.8	2.5	2.0	9.7
1974	-3.6	2.5	6.4	7.7	13.3	17.6	18.8	18.5	15.1	15.0	6.5	1.7	10.0
1975	1.0	0.7	7.3	11.8	13.9	18.1	20.5	19.4	15.8	11.1	5.8	-1.3	10.3
1976	-1.2	-1.1	3.8	9.7	13.0	15.7	18.8	17.0	14.3	12.8	7.6	2.7	9.4
1977	1.0	6.5	4.8	9.2	14.0	16.9	19.3	18.7	15.5	8.6	9.1	0.9	10.4
1978	-0.2	5.6	6.4	8.7	14.0	17.0	19.1	17.3	15.1	11.6	4.6	3.1	10.2
1979	2.0	4.4	7.0	8.9	13.9	17.9	17.9	19.2	16.1	11.2	7.2	3.0	10.7
1980	-0.9	0.2	4.0	8.4	14.3	17.6	20.4	19.6	14.0	12.7	7.8	4.1	10.2
1981	3.0	2.2	6.3	8.7	11.7	18.6	19.5	19.1	16.5	14.2	5.1	7.0	11.0
1982	1.3	-1.0	3.4	9.9	13.0	17.3	17.0	18.4	17.2	11.4	4.4	4.3	9.7
1983	-2.0	0.9	5.5	11.0	14.4	16.1	19.0	17.4	15.9	9.9	5.6	3.8	9.8
1984	2.9	3.4	5.3	7.5	15.0	16.4	18.0	16.7	17.5	12.2	6.9	0.4	10.2
1985	3.3	-3.7	3.3	10.1	15.5	16.6	17.5	20.6	14.7	9.0	9.3	2.2	9.9
1986	4.0	3.7	5.2	12.0	10.9	16.9	19.5	21.1	17.1	10.6	3.2	1.6	10.5
1987	1.5	3.8	0.8	7.3	13.6	16.9	20.8	18.6	16.5	10.6	6.7	2.7	10.0
1988	2.2	2.7	4.8	9.9	13.8	16.6	20.4	19.9	15.5	9.9	3.8	3.2	10.2
1989	-2.9	0.7	7.5	14.4	13.6	16.8	19.3	20.7	15.6	10.5	5.8	1.4	10.3
1990	-2.8	2.2	5.8	9.7	12.7	16.9	20.1	18.9	15.3	12.2	8.8	3.2	10.3
Average	0.7	1.8	4.8	9.7	13.7	17.1	19.4	19.2	15.7	11.3	6.7	2.8	10.2

Table 6-15 Estimated Monthly Mean Temperature on Reservoir Surface (EL. 437m)

Unit: mm

Year	Jan.	Feb.	March	Apr.	May	June	July	Aug.	Sept.	Oct.	Nov.	Dec.	Average
1956	3.9	2.5	2.2	12.0	13.6	18.5	20.6	22.3	15.3	11.4	4.7	-1.0	10.5
1957	-0.7	4.8	5.6	11.3	14.4	19.6	22.4	22.8	19.7	14.8	8.7	3.9	12.3
1958	2.9	7.2	7.1	10.4	17.3	18.7	20.4	21.3	16.1	12.5	7.5	5.7	12.3
1959	3.8	-4.6	3.2	10.7	14.6	17.7	21.3	20.6	14.4	10.1	7.7	7.1	10.6
1960	2.7	2.5	5.7	10.5	16.5	17.9	20.4	19.9	17.1	15.0	10.4	7.7	12.2
1961	0.8	2.6	5.5	13.2	15.7	18.8	20.9	21.1	15.6	12.6	8.6	4.9	11.7
1962	4.1	3.0	9.1	10.4	16.6	19.0	21.8	22.7	17.9	14.0	12.9	6.0	13.2
1963	2.9	7.2	4.7	9.4	14.3	19.0	21.4	22.4	18.4	13.4	8.9	4.6	12.2
1964	1.5	0.4	6.6	10.1	13.7	18.7	20.7	19.2	16.6	13.1	7.7	6.0	11.2
1965	3.0	0.6	6.9	9.7	15.3	19.8	20.4	19.7	17.9	9.7	8.8	7.2	11.6
1966	4.4	7.9	7.0	12.5	14.5	18.2	22.3	21.8	17.0	15.6	12.2	4.7	13.2
1967	0.7	-0.7	4.7	10.9	14.7	17.3	20.5	21.0	17.1	13.6	6.3	5.1	11.0
1968	0.9	1.6	4.9	12.8	17.6	18.0	20.9	19.9	17.0	11.9	9.2	5.2	11.7
1969	1.5	4.0	5.8	8.3	16.8	20.2	19.1	22.1	18.2	11.7	8.7	7.4	12.0
1970	5.3	6.3	8.8	13.6	14.1	18.2	22.1	20.4	16.6	11.5	9.3	1.2	12.3
1971	6.9	3.7	7.6	10.5	15.6	18.0	20.7	20.5	17.8	10.5	8.5	1.6	11.9
1972	-3.0	1.2	5.6	13.9	15.7	19.1	21.3	21.0	17.5	12.7	7.9	1.0	11.2
1973	-0.4	6.3	5.2	10.6	15.4	17.6	21.2	19.5	18.1	13.3	4.0	3.5	11.2
1974	-2.1	4.0	7.9	9.2	14.8	19.1	20.3	20.0	16.6	16.5	8.0	3.2	11.5
1975	2.5	2.2	8.8	13.3	15.4	19.6	22.0	20.9	17.3	12.6	7.3	0.2	11.9
1976	0.3	0.4	5.3	11.2	14.5	17.2	20.3	18.5	15.8	14.3	9.1	4.2	11.0
1977	2.5	8.0	6.3	10.7	15.5	18.4	20.8	20.2	17.0	10.1	10.6	2.4	11.9
1978	1.3	7.1	7.9	10.2	15.5	18.5	20.6	18.8	16.6	13.1	6.1	4.6	11.7
1979	3.5	5.9	8.5	10.4	15.4	19.4	19.4	20.7	17.6	12.7	8.7	4.5	12.3
1980	0.6	1.7	5.5	9.9	15.8	19.1	21.9	21.1	15.5	14.2	9.3	5.6	11.7
1981	4.5	3.7	7.8	10.2	13.2	20.1	21.0	20.6	18.0	15.7	6.6	8.5	12.5
1982	2.8	0.5	4.9	11.4	14.5	18.8	18.5	19.9	18.7	12.9	5.9	5.8	11.2
1983	-0.5	2.4	7.0	12.5	15.9	17.6	20.5	18.9	17.4	11.4	7.1	5.3	11.3
1984	4.4	4.9	6.8	9.0	16.5	17.9	19.5	18.2	19.0	13.7	8.4	1.9	11.7
1985	4.8	-2.2	4.8	11.6	17.0	18.1	19.0	22.1	16.2	10.5	10.8	3.7	11.4
1986	5.5	5.2	6.7	13.5	12.4	18.4	21.0	22.6	18.6	12.1	4.7	3.1	12.0
1987	3.0	5.3	2.3	8.8	15.1	18.4	22.3	20.1	18.0	12.1	8.2	4.2	11.5
1988	3.7	4.2	6.3	11.4	15.3	18.1	21.9	21.4	17.0	11.4	5.3	4.7	11.8
1989	-1.4	2.2	9.0	15.9	15.1	18.3	20.8	22.2	17.1	12.0	7.3	2.9	11.8
1990	-1.3	3.7	7.3	11.2	14.2	18.4	21.6	20.4	16.8	13.7	10.3	4.7	11.8
Average	2.2	3.3	6.3	11.2	15.2	18.6	20.9	20.7	17.2	12.8	8.2	4.3	11.7

Table 6-16 Estimated Monthly Total Evaporation from Reservoir Surface

Unit: mm

Year	Jan.	Feb.	March	Apr.	May	June	July	Aug.	Sept.	Oct.	Nov.	Dec.	Total
1956	8.6	0.0	0.0	62.8	73.6	106.4	120.5	131.9	85.0	58.8	13.9	0.0	661.4
1957	0.0	14.6	20.0	58.2	78.9	113.8	132.5	135.2	114.4	81.6	40.7	8.6	798.5
1958	1.9	30.7	30.0	52.1	98.4	107.7	119.1	125.2	90.3	66.2	32.7	20.6	774.9
1959	7.9	0.0	3.9	54.1	80.3	101.0	125.2	120.5	78.9	50.1	34.0	30.0	686.0
1960	0.5	0.0	20.6	52.8	93.0	102.4	119.1	115.8	97.0	82.9	52.1	34.0	770.4
1961	0.0	0.0	19.3	70.9	87.6	108.4	122.5	123.8	87.0	66.9	40.1	15.3	741.7
1962	9.9	2.5	43.4	52.1	93.7	109.8	128.5	134.5	102.4	76.2	68.9	22.6	844.6
1963	1.9	30.7	13.9	45.4	78.3	109.8	125.8	132.5	105.7	72.2	42.1	13.3	771.6
1964	0.0	0.0	26.7	50.1	74.2	107.7	121.1	111.1	93.7	70.2	34.0	22.6	711.6
1965	2.5	0.0	28.7	47.4	85.0	115.1	119.1	114.4	102.4	47.4	41.4	30.7	734.2
1966	11.9	35.4	29.3	66.2	79.6	104.4	131.9	128.5	96.4	87.0	64.2	13.9	848.6
1967	0.0	0.0	13.9	55.5	80.9	98.4	119.8	123.2	97.0	73.6	24.7	16.6	703.5
1968	0.0	0.0	15.3	68.2	100.4	103.1	122.5	115.8	96.4	62.2	44.1	17.3	745.1
1969	0.0	9.2	21.3	38.1	95.0	117.8	110.4	130.5	104.4	60.8	40.7	32.0	760.3
1970	18.0	24.7	41.4	73.6	76.9	104.4	130.5	119.1	93.7	59.5	44.8	0.0	786.5
1971	28.7	7.2	33.4	52.8	87.0	103.1	121.1	119.8	101.7	52.8	39.4	0.0	746.9
1972	0.0	0.0	20.0	75.6	87.6	110.4	125.2	123.2	99.7	67.5	35.4	0.0	744.5
1973	0.0	24.7	17.3	53.5	85.6	100.4	124.5	113.1	103.7	71.6	9.2	5.9	709.4
1974	0.0	9.2	35.4	44.1	81.6	110.4	118.5	116.5	93.7	93.0	36.0	3.9	742.2
1975	0.0	0.0	41.4	71.6	85.6	113.8	129.9	122.5	98.4	66.9	31.4	0.0	761.3
1976	0.0	0.0	18.0	57.5	79.6	97.7	118.5	106.4	88.3	78.3	43.4	10.6	698.2
1977	0.0	36.0	24.7	54.1	86.3	105.7	121.8	117.8	96.4	50.1	53.5	0.0	746.4
1978	0.0	30.0	35.4	50.8	86.3	106.4	120.5	108.4	93.7	70.2	23.3	13.3	738.2
1979	5.9	22.0	39.4	52.1	85.6	112.4	112.4	121.1	100.4	67.5	40.7	12.5	772.3
1980	0.0	0.0	19.3	48.8	88.3	110.4	129.2	123.8	86.3	77.6	44.8	20.0	748.4
1981	12.6	7.2	34.7	50.8	70.9	117.1	123.2	120.5	103.1	87.6	26.7	39.4	793.7
1982	1.2	0.0	15.3	58.8	79.6	108.4	106.4	115.8	107.7	68.9	22.0	21.3	705.4
1983	0.0	0.0	29.3	66.2	89.0	100.4	119.8	109.1	99.0	58.8	30.0	18.0	719.6
1984	11.9	15.3	28.0	42.7	93.0	102.4	113.1	104.4	109.8	74.2	38.7	0.0	733.5
1985	14.6	0.0	14.6	60.2	96.4	103.7	109.8	130.5	91.0	52.8	54.8	7.2	735.5
1986	19.3	17.3	27.3	72.9	65.5	105.7	123.2	133.9	107.1	63.5	13.9	3.2	752.8
1987	2.5	18.0	0.0	41.4	83.6	105.7	131.9	117.1	103.1	63.5	37.4	10.6	714.8
1988	7.2	10.6	24.7	58.8	85.0	103.7	129.2	125.8	96.4	58.8	18.0	13.9	732.0
1989	0.0	0.0	42.7	89.0	83.6	105.1	121.8	131.2	97.0	62.8	31.4	1.9	766.5
1990	0.0	7.2	31.4	57.5	77.6	105.7	127.2	119.1	95.0	74.2	51.5	13.9	760.3
Average	4.8	10.1	24.6	57.3	84.4	106.8	122.2	121.2	97.6	67.9	37.1	13.5	747.5

6.4 Sedimentation in Reservoir

6.4.1 Data Used for Calculation of Sediment Volume

Sediment transported down a stream is divided into suspended load and bed load according to the mode in which the sediment is carried down. Of the two, the measurement technique for suspended load has been established, and in Turkey, continuous observations of suspended loads in rivers are being conducted by EIE. On the other hand, with regard to bed load, measurement in a stream is difficult, and it cannot be avoided making only estimates of volumes.

The design sedimentation at a reservoir can be calculated using sedimentation data of an existing reservoir in the same river basin, or from observation data of suspended load in the vicinity of the project site.

In the Devrek River basin there is Gölköy Dam near Bolu, but since water is conducted to the reservoir through canals from intake weirs, the sedimentation data in the reservoir are not serviceable as data for calculation of the design sedimentation. Consequently, design sedimentiation of reservoir was estimated by using observation data on suspended loads.

In the Filyos River basin, EIE is making measurements of suspended loads at Gauging Station No.1335 on the Filyos River, Gauging Station No.1314 on the Yenice River, and Gauging Station No.1334 on the Büyüksu River, a tributary of the Devrek River on which the project site is located (See Table 6-17). Further, EIE has been analyzing measurement values from gauging stations throughout Turkey, calculated correlation equations for river runoff and daily suspended load and annual sedimentation per square kilometer, and compiles these results every 5 years as Sediment Data and Sediment Transport Amounts for Surface Waters in Turkey.

The data on suspended load from observations being carried out by EIE were used for calculation of design sedimentation in the reservoir at the project site.

6.4.2 Suspended Load

The sedimentation at the Köprübaşı damsite was estimated by the four methods as shown below and the value to be adopted decided upon carrying out examinations.

(1) Observation Data

According to Sediment Data and Sediment Transport Amounts for Surface Waters in Turkey published in 1987 by EIE, annual suspended loads per square kilometer based on data up to 1984 are the following:

Station	Catchment Area (km^2)	Period	Amount ($t/yr/km^2$)
No. 1314	5,086.8	1973-84	182
No. 1334	1,102.0	1978-84	33
No. 1335	13,300.4	1967-84	286

Of them, regarding Gauging Station No.1334 with a comparatively short observation period, the annual suspended load per square kilometer was reexamined based on observation data of EIE. With X as runoff (m^3/s), Y as daily suspended load (ton/day), and observation period taken from November 1977 to December 1990, the relationship of X and Y was as below (see Figure 6-16).

$$\log Y = 0.4907*(\log X)^2 + 0.8583 * \log X + 0.6081$$
$$R = 0.877$$

The annual suspended load per square kilometer at Gauging Station No.1334 was calculated from the above equation and

daily runoff of the water years 1967 to 1989, and it was 39 ton/year/km^2.

(2) Proposition 1: Same Calculation Method as That in Master Plan Report

The annual suspended load at Gauging Station No.1311, downstream of the project site, was to be taken as 182 ton/year/km^2, the same as that at Gauging Station No.1314 on the Soğanlı River. In this case the annual suspended load $q_{s(Rest)}$ of the Devrek River, Mengen River, and Büyüksu River downstream of Gauging Station No.1334 was as below.

$$q_{s(Rest)} = [182 * A_{(No.1311)} - 39 * A_{(No.1334)}] / [A_{(No.1311)} - A_{(No.1334)}]$$

where, $A_{(No.1311)}$: Catchment area of Gauging Station No. 1311, 2,420.0 km^2

$A_{(No.1334)}$: Catchment area of Gauging Station No.1334, 1,102.0 km^2

Consequently $q_{s(Rest)}$ was 302 ton/year/km^2. Hence, the annual suspended loads at the upstream and Master Plan damsites were obtained as follows:

Upstream damsite:

Q_{SUD} = 301,790 ton/year (154 ton/year/km^2)

Master Plan damsite:

Q_{SMD} = 312,360 ton/year (157 ton/year/km^2)

(3) Propostion 2: Calculation by Using Weighted Average on Annual Suspended Load per km^2

Average annual spsended load per square kilometer in the project area was estimated by using average on those of

No.1314 and No.1334 stations weighted with catchment areas of the stations.

$$q_{s(AV)} = [182 \times A_{(No.1314)} + 39\ A_{(No.1334)}] / [A_{(No.1314)} + A_{(No.1334)}]$$

where, $q_{s(AV)}$: Weighted average on annual suspended load (ton/year/km^2)

$A_{(No.1314)}$: Catchment area of No.1314 station (km^2)

$A_{(No.1334)}$: Catchment area of No.1334 station (km^2)

As result, $q_{s(AV)}$ = 157 ton/year/km^2 was obtained, and annual suspended loads at upstream and Master Plan damsites are as below.

Upstream damsite:

Q_{SUD} = 307,560 ton/year (157 ton/year/km^2)

Master Plan damsite:

Q_{SMD} = 313,060 ton/year (157 ton/year/km^2)

(4) Proposition 3: Calculation from Relationship of Catchment Area and Annual Suspended Load

EIE is carrying out observations of suspended load at five gauging stations in the Region 13, including the abovementioned three gauging stations in the Filyos River basin. The catchment areas and annual suspended loads of these five gauging stations can be expressed by the relationship below (see Figure 6-17).

$$\log Y = 1.2208 * \log X + 1.2693$$

where, Y: Annual suspended load at gauging station (ton/year)

X: Catchment area of gauging station (km^2)

The correlation coefficient (R) became 0.935. With this equation, the annual suspended loads at the upstream and Master Plan damsites are obtained as follows:

Upstream damsite:

Q_{SUD} = 194,180 ton/year (99 ton/year/km^2)

Master Plan damsite:

Q_{SMD} = 198,430 ton/year (100 ton/year/km^2)

(5) Proposition 4: Calculation from Empirical Equation

Some empirical equations have been proposed based on observations of suspended loads at many rivers and streams, and these are used when observation values on suspended load of a river are not available.

Fleming expressed the relationship between average annual runoff and annual suspended load by the following equation:

$$Q_s = aQ^n$$

where, Q: Average annual runoff (cu.ft/s)
Q_s: Average annual suspended load (ton/year)
a, n: Coefficients depending on vegetation in basin
Area of mixed broad-leafed and coniferous trees;
n = 1.02, a = 106
Area of coniferous trees and tall grasses;
n = 0.82, a = 3,196

Taking into consideration the vegetation in the Devrek River basin, the annual suspended loads at the upstream and Master Plan damsites are estimated to be as follows:

Upstream damsite:

Q_{SUD} = 305,520 ton/year (156 ton/year/km^2)

Master Plan damsite:

Q_{SMD} = 307,150 ton/year (154 ton/year/km^2)

(6) Suspended Load to be Adopted

The following compiles the above results.

(Unit: ton/year/km^2)

Method	Upstream Damsite	Master Plan Damsite
Proposition 1: Same Calculation Method as That in Master Plan Report	154	157
Proposition 2: Calculation by Using Weighted Average on Suspended Load per km^2	157	157
Proposition 3: Calculation from Relationship of Catchment Area and Annual Suspended Load	99	100
Proposition 4: Calculation from Empirical Equation	156	154

The calculation results of the propositions 1 and 2 were approximately same value, and were almost equal to the results of the proposition 4 in which an empirical equation was used. Consequently, 157 ton/year/km^2 was adopted as annual suspended load per square kilometer at both upstream and Master Plan damsites. Annual suspended load at each damsite was as below.

Upstream damsite: 307,506 ton/year
Master Plan damsite: 313,060 ton/year

On the other hand, according to DSI, though annual suspended loads obtained at No.1334 and No.1314 stations are reasonable taking into account vegetation in the Devrek and Soğanlı River basins, it is proposed that 182 ton/year/km^2 including 20% of suspended load as bed load should be adopted as conservative estimate on sedimentation

in reservoir. In this case, suspended load is estimated as below.

$$\text{Suspended load (ton/year/km}^2\text{)} = 182 \times 1/1.2 = 152$$

This value is nearly equal to that adopted above.

6.4.3 Bed Load

Because a measurement method for bed load volume is not established, and the volume is generally expressed in terms of a ratio of suspended load volume, it was assumed that bed load equals 20% of suspended load.

6.4.4 Trap Efficiency of Reservoir

Brune gave the relationship between "total storage volume/annual inflow" and trap efficiency. When total storage volume of reservoir of each dam is taken to be 200×10^6 m^3, values of the "total storage volume/annual inflow" were as follows:

Upstream damsite: $200 \times 10^6/445.90 \times 10^6 = 44.8\%$
Master Plan damsite: $200 \times 10^6/453.86 \times 10^6 = 44.1\%$

Consequently, the trap efficiency of each reservoir was obtained as 100% from the Brune's diagram by using these values.

6.4.5 Calculation of Sediment (by Weight) Entering Reservoir

By using the abovementioned suspended load volume, bed load volume (%), and trap efficiency, and with the period of sedimentation as 50 years, the sedimentation volumes at the reservoirs of the upstream and Master Plan damsites were obtained as follows:

$$S_w = Q_s \times (1 + Eb/100) \times E_b/100 \times T$$

where, S_w: Reservoir sedimentation at T years (ton)
Q_s: Annual suspended load (ton/year)
E_b: Bed load ratio (%)
E_t: Trap efficiency (%)
T: Period (year)

Upstream damsite:

S_{WU} = 307,560 ton/year x 1.2 x 50 year
= 18.45×10^6 ton

Master Plan damsite:

S_{WM} = 313,060 ton/year x 1.2 x 50 year
= 18.78×10^6 ton

6.4.6 Sediment Density

The average sediment density W_t after elapse of t years of the sediment deposited inside a reservoir would be calculated by the following equation of Lone and Koelzer:

$$W_t = W_1 + K \log t$$

Accordingly, the density W_T of sediment in the reservoir after T years would be calculated by the equation below on integrating the above equation:

$$W_T = W_1 + 0.4343 * K * T/(T-1) * (\ln T-1)$$

where, W_1: Initial density (ton/m^3)
K : Density increase coefficient (ton/m^3)
T : Calculation period (year)

For initial density W_1 and density increase coefficient K, the values below are employed taking into consideration the

components of the sediment and operating conditions of the reservoir.

	Sand	Silt	Clay
Rate (%)	40	30	30
W_1 (t/m^3)	1.490	1.041	0.48
K (t/m^3)	0	0.0913	0.256

As a consequence of the above, W_{50} was obtained as 1.19 t/m^3.

6.4.7 Design Sedimentation of Reservoir

The sedimentation volume S_v(m^3) after 50 years in each reservoir was as follows:

$$S_V = S_W / W_{50}$$

Upstream damsite:

$$S_{VU} = 18.45 \times 10^6 \text{ ton}/1.19 \text{ ton/m}^3 = 15.50 \times 10^6 \text{ m}^3$$

Master Plan damsite:

$$S_{VM} = 18.78 \times 10^6 \text{ ton}/1.19 \text{ ton/m}^3 = 15.78 \times 10^6 \text{ m}^3$$

Accordingly, assuming that the sediment surface of the reservoir 50 years later is horizontal, the elevations were determined as follows from the capacity curve of each reservoir:

Upstream damsite: EL.388.40 m
Master Plan damsite: EL.380.40 m

Decrease amount of annual suspended loads (ΔQs) at the Filyos river mouth can be estimated with annual suspended loads per km^2 at No. 1335 gauging station (see 6.4.2 (1)) and annual suspended loads at the dam site decided in 6.4.2 (6).

$$\Delta Qs = 313{,}060 \text{ ton/year}/(286 \text{ ton/year/km}^2 \times 13{,}300 \text{ km}^2)$$
$$= 0.082$$

The decrease amount is assumed to be around 8%, and it is considered that the decrease amount will be small.

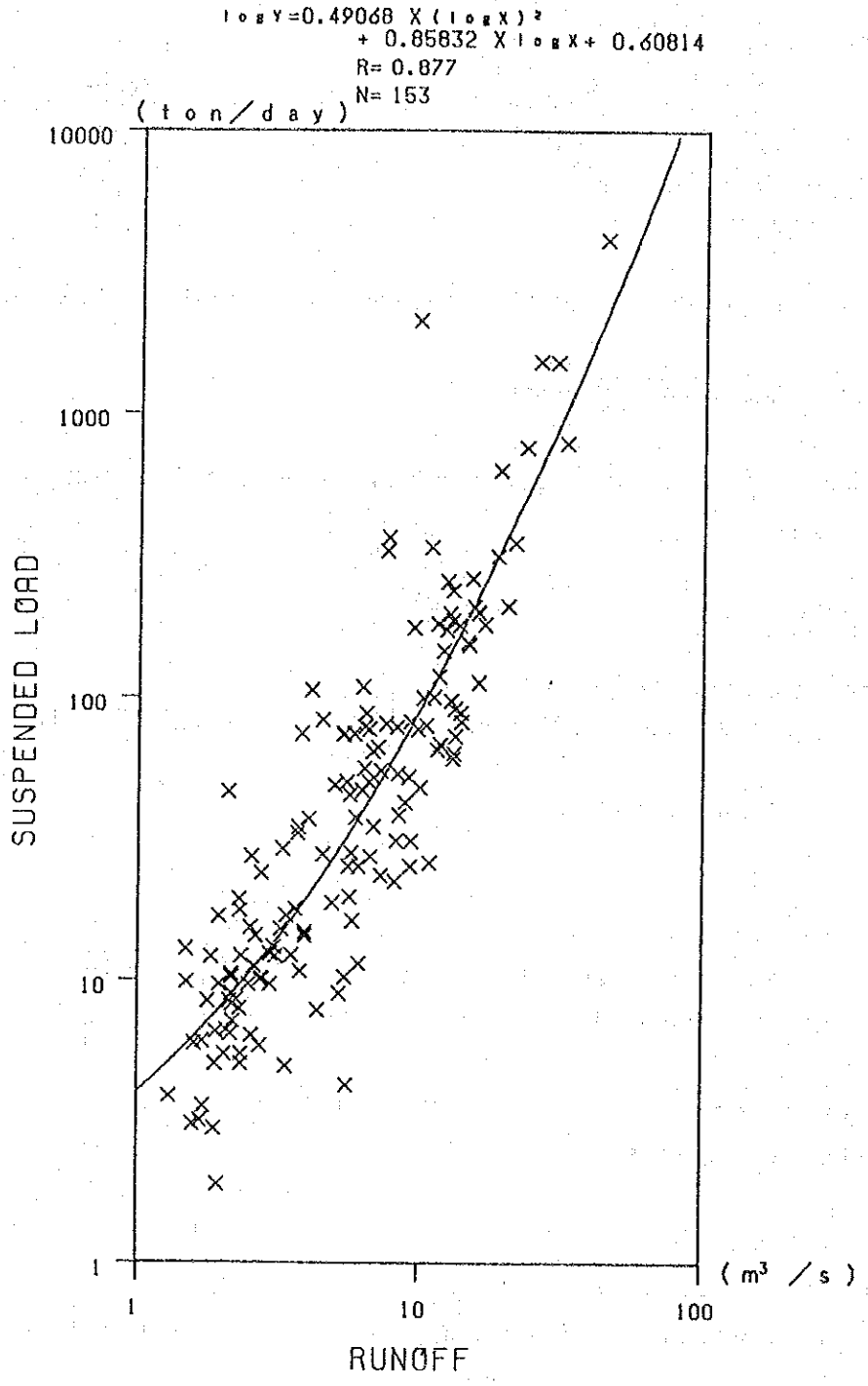

Figure 6-16 Correlation between Runoff and Suspended Load at No.1334 G.S.

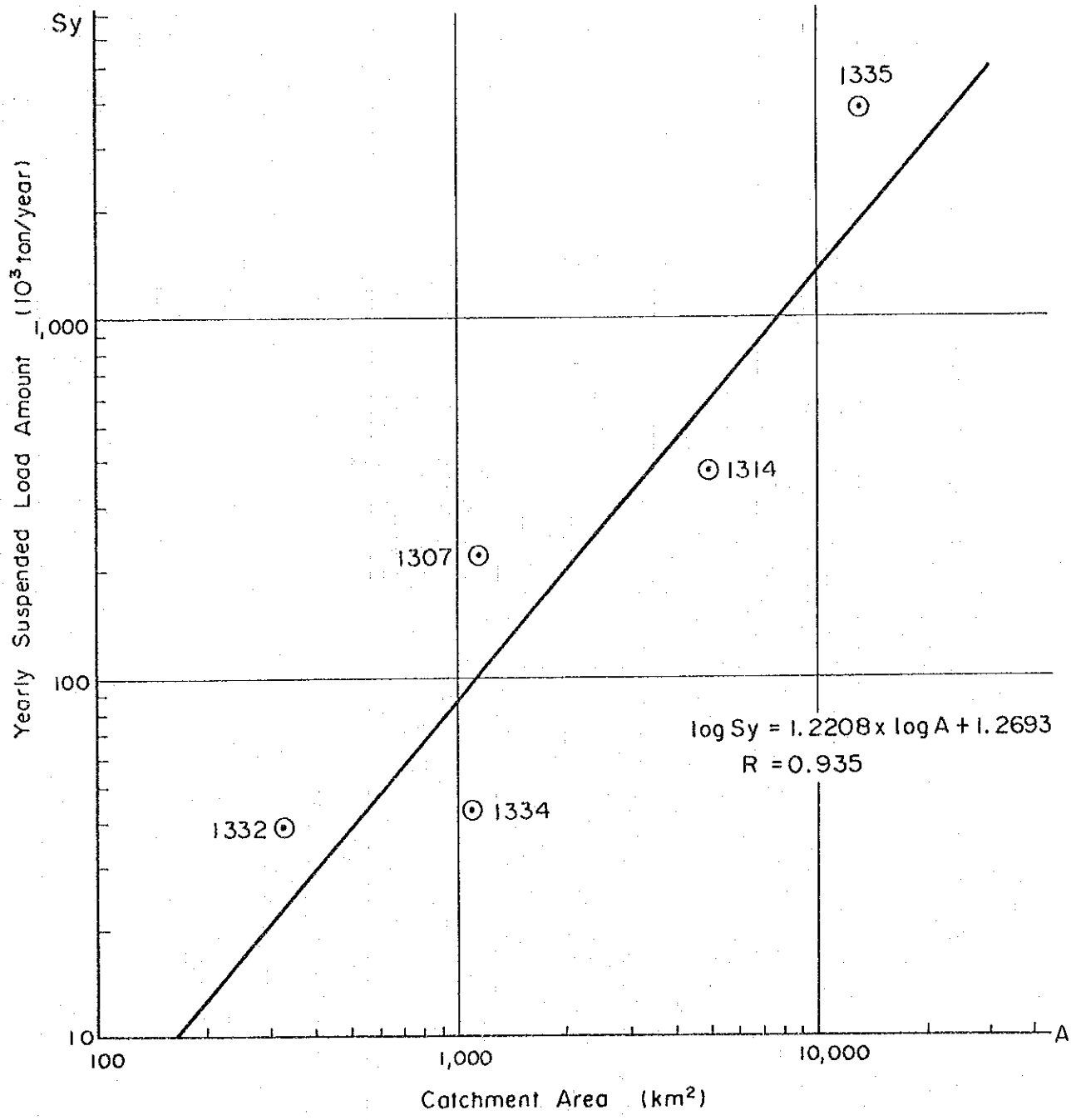

Figure 6-17 Correlation between Catchment Area and Yearly Suspended Load Amount

Table 6-17 List of Gauging Stations Observing Suspended Load in Filyos River Basin

Station No.	Station Name	River	Catchment Area (km²)	Observation Period (Water Year) 1960	70	80	90	Remarks
1 3 1 4	Karabük	Soganli	5,086.8	1963	1973			
1 3 3 4	Beşedeğirmenler	Büyüksu	1,120.0	1967	1978			
1 3 3 5	Derecikviran	Filyos	13,300.4	1967 1964				

Note : ═══ Measurement for Suspended Load

——— Measurement for Runoff

6.5 Probable Flood Discharge

6.5.1 Data used for Calculation of Probable Flood Discharge

Of the six gauging stations in the catchment of the project site and its surrounding area, peak discharges during floods are being observed at five gauging stations except No.13-44 gauging station. Table 6-18 shows annual maximum peak discharges at the five gauging stations and annual maximum daily discharges at No.13-44 gauging station. Calculation of probable floods was carried out by using the discharges at No.1319 and No.1334 gauging stations of which observation periods are relatively long, compared with periods of the other three gauging stations. The logarithmic normal distribution, Gumbel distribution and Logarithmic Pearson III distribution were adopted as probable disbribution functions, after skewness and kurtosis of discharges at the two gauging stations were calculated respectively.

6.5.2 Probable Flood Discharge at Damsite

The calculation results of probable flood discharges using the three before-mentioned distributions are shown in Figures 6-18 and 6-19, and Table 6-19.

Probable flood discharge of each return period at the damsite was calculated as summation among discharges of the two gauging stations and discharge in the residual area of catchment area of the two gauging stations. Discharges in the residual area were estimated by multiplying the area (km^2) by flood discharge per square kilometer at No.1319 gauging station, because flood discharge per square kilometer at No.1319 gauging station was larger than that of No.1334 gauging station. Table 6-20 shows these results.

It is considered that the Gumbel distribution gave the best fitness of the above three, and for capacity calculation of the diversion tunnel the result of the distribution was applied.

Figure 6-18 Flood Frequency at No.1319 G.S.

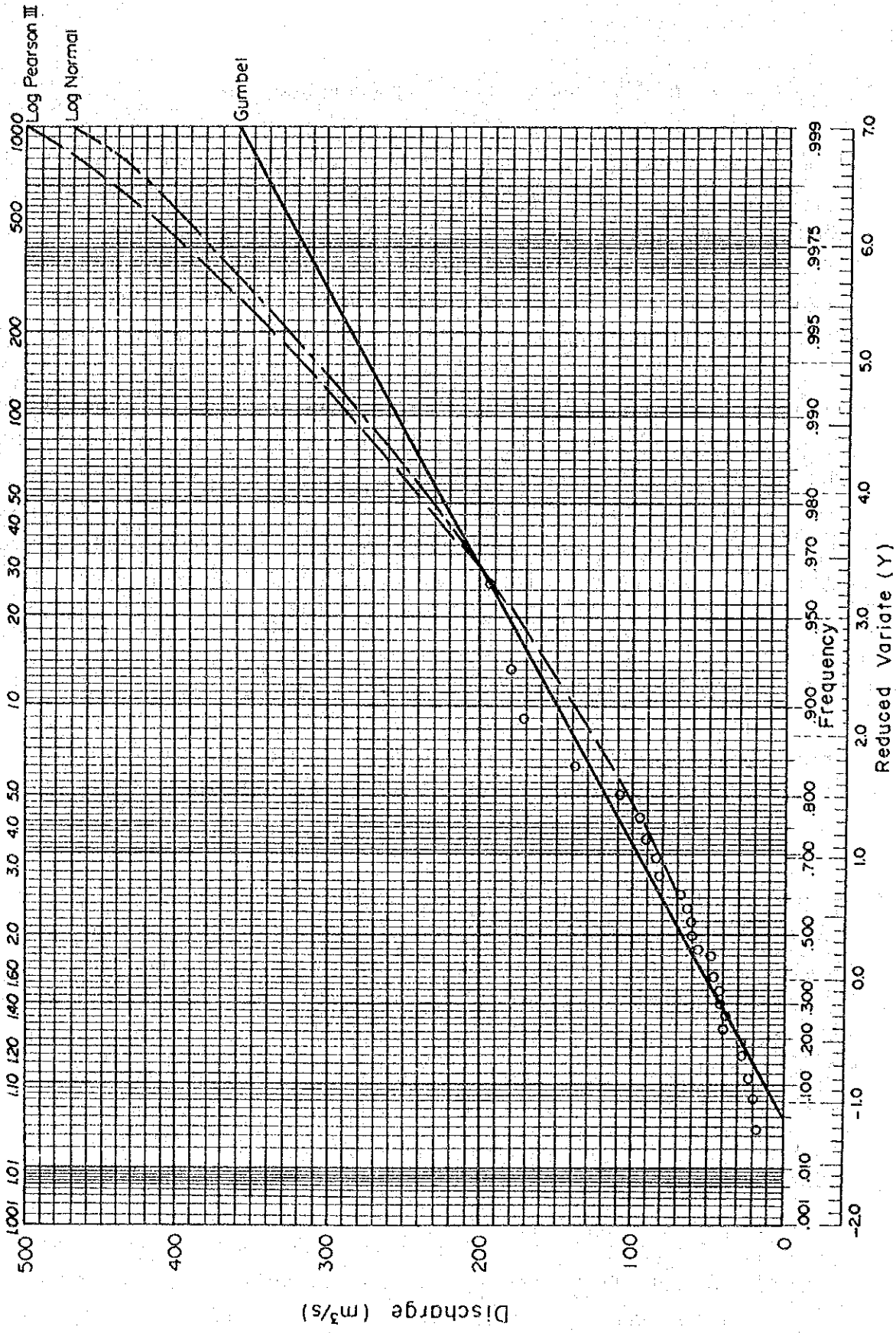

Figure 6-19 Flood Frequency at No.1334 G.S.

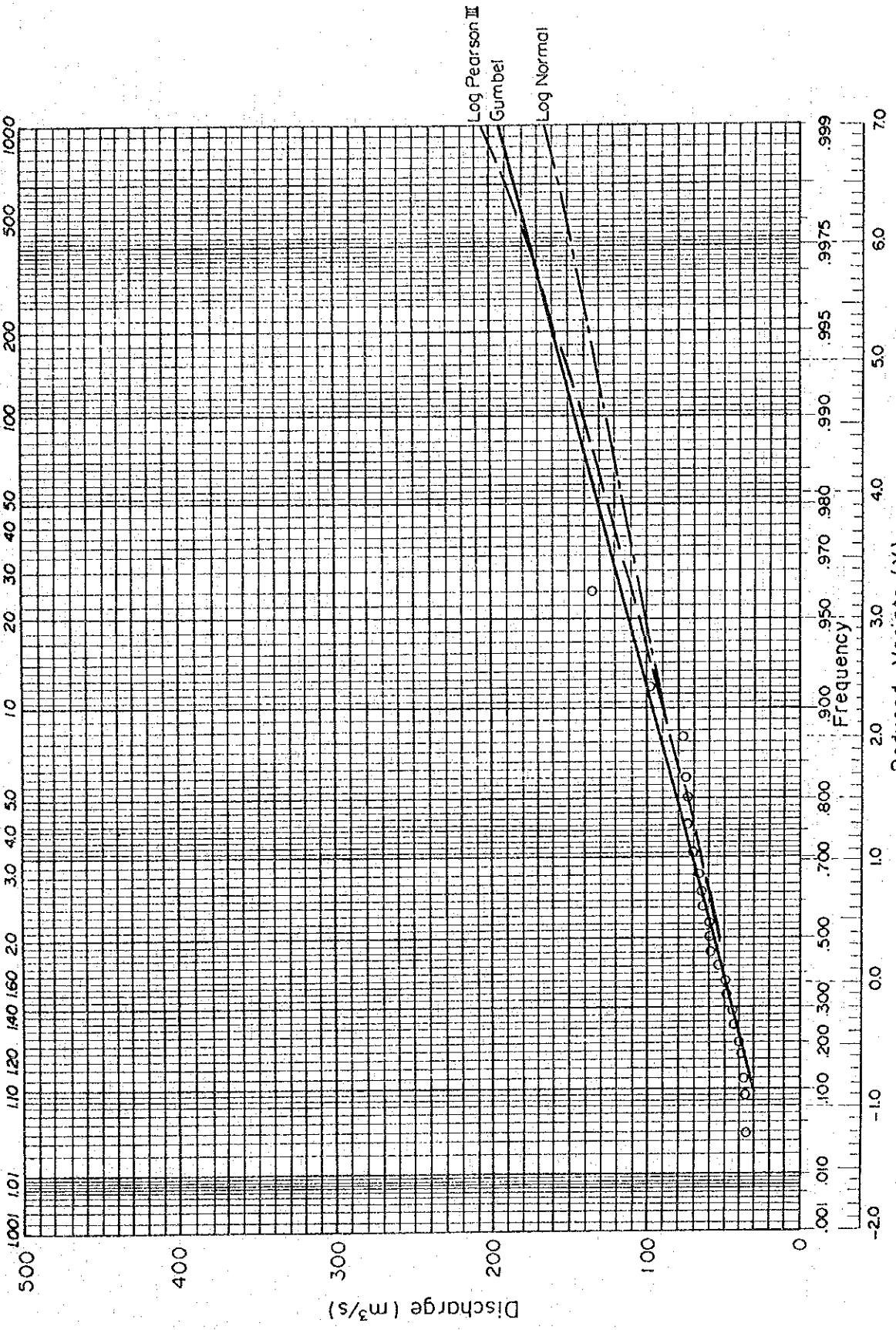

Table 6-18 Yearly Peak Discharge at Gauging Stations in the Project Area and Vicinity

Water Year	No. 1308		No. 1311		No. 1318		No. 1319		No. 1334		No. 13-44	
	Date	Peak Run-off	Date	Peak Run-off	Date	Peak Run-off	Date	Peak Run-off	Date	Peak Run-off	Date	Max. Daily Run-off
1954	Mar. 1954	57.0										
1955	Aug. 1955	25.5										
1956	Feb. 1956	83.5										
1957	May 1957	55.0										
1958	Mar. 1958	73.8	Mar. 1958	119.8								
1959	Mar. 1959	92.2	16 Mar. 1959	163.6								
1960	2 Feb. 1960	65.2	21 Feb. 1960	81.2								
1961	29 Dec. 1960	55.3	24 Mar. 1961	83.6								
1962	7 Mar. 1962	47.5	3 Apr. 1962	184								
1963			24 May 1963	327								
1964			14 Dec. 1964	130								
1965			14 July 1965	166	12 Apr. 1965	185	14 Apr. 1965	41.8				
1966			13 Apr. 1966	76.2	13 Apr. 1966	59.5	13 Apr. 1966	19.5				
1967			3 Apr. 1967	94.0	16 Mar. 1967	72.1	5 May 1967	42.8	24 Apr. 1967	37.2		
1968			13 Mar. 1968	231	13 Mar. 1968	215	18 Feb. 1968	62.1	12 Mar. 1968	71.0		
1969			27 Apr. 1969	155	27 Apr. 1969	149	28 Apr. 1969	61.1	27 Apr. 1969	65.5		
1970			13 Feb. 1970	144	13 Feb. 1970	137	31 Mar. 1970	18.2	12 Feb. 1970	76.5		
1971			11 June 1971	162	18 May 1971	136	18 May 1971	68.3	10 June 1971	60.0		
1972							22 June 1972	171.0	23 June 1972	135.0		
1973							26 Oct. 1973	28.7	26 Oct. 1972	44.0		
1974							12 May 1974	38.8	18 Mar. 1974	68.0		
1975							1 May 1975	182.0	1 May 1975	98.0		
1976							27 Mar. 1976	28.7	20 Dec. 1975	75.0		
1977							25 Mar. 1977	23.2	13 Dec. 1976	49.3		
1978							9 Apr. 1978	95.9	9 Apr. 1978	45.2		
1979							2 June 1979	192.0	2 June 1979	56.7		
1980							27 Mar. 1980	60.7	28 Mar. 1980	74.2		
1981							14 Mar. 1981	108.0	15 Mar. 1981	77.2		
1982							13 Jan. 1982	91.2	13 Jan. 1982	60.4		
1983							28 July 1983	82.4	29 July 1983	36.0	28 July 1983	220
1984							16 Apr. 1984	139.0	16 Apr. 1984	50.0	17 Apr. 1984	260
1985							18 Mar. 1985	57.2	16 Mar. 1985	37.4	13 Feb. 1985	175
1986							15 May 1986	49.1	17 Jan. 1986	40.0	28 Dec. 1985	180
1987							30 Jan. 1987	39.5	30 Jan. 1987	64.4	31 Jan. 1987	260
1988							10 Dec. 1987	47.3	10 Dec. 1987	38.9	10 Dec. 1987	120
1989							28 Feb. 1989	86.4	27 Feb. 1989	59.8	1 Mar. 1989	200
1990											7 May 1990	130
1991											7 July 1991	420
1992											29 Mar. 1992	240

Table 6-19 Probable Flood at No. 1319 and No. 1334 G.Ss

(1) No. 1319 Gauging Station

Return Period (Years)	Log Normal Distribution		Gumbel Distribution		Log Pearson Type III Distribution	
	Discharge (m^3/s)	Discharge per km^2 ($m^3/s/km^2$)	Discharge (m^3/s)	Discharge per km^2 ($m^3/s/km^2$)	Discharge (m^3/s)	Discharger per km^2 ($m^3/s/km^2$)
2	59	0.08	66	0.09	59	0.09
5	104	0.14	117	0.15	104	0.14
10	140	0.18	151	0.20	141	0.18
25	194	0.25	194	0.25	195	0.25
50	235	0.31	226	0.29	241	0.31
100	282	0.37	257	0.34	291	0.38
1,000	470	0.61	361	0.47	502	0.66
10,000	716	0.93	465	0.61	810	1.06

(2) No. 1334 Gauging Station

Return Period (Years)	Log Normal Distribution		Gumbel Distribution		Log Pearson Type III Distribution	
	Discharge (m^3/s)	Discharge per km^2 ($m^3/s/km^2$)	Discharge (m^3/s)	Discharge per km^2 ($m^3/s/km^2$)	Discharge (m^3/s)	Discharger per km^2 ($m^3/s/km^2$)
2	58	0.05	58	0.05	57	0.05
5	77	0.07	82	0.07	77	0.07
10	90	0.08	97	0.09	91	0.08
25	105	0.10	117	0.11	110	0.10
50	116	0.11	131	0.12	126	0.11
100	127	0.12	146	0.13	143	0.13
1,000	164	0.14	193	0.18	206	0.19
10,000	203	0.18	240	0.22	265	0.24

Table 6-20 Probable Flood at Dam Site

(1) Master Plan Dam Site

Unit: m^3/S

Return Period (Years)	Log Normal Distribution	Gumbel Distribution	Log Pearson Type III Distribution
2	127	135	125
5	198	218	198
10	253	273	255
25	331	342	337
50	390	394	406
100	455	445	482
1,000	711	613	791
10,000	1,036	782	1,208

(2) Upper Dam Site

Unit: m^3/S

Return Period (Years)	Log Normal Distribution	Gumbel Distribution	Log Pearson Type III Distribution
2	124	132	123
5	193	213	193
10	247	266	248
25	322	333	328
50	379	383	395
100	442	433	468
1,000	690	597	768
10,000	1,004	761	1,171

Note: $Q_P = Q_{P(1319)} + Q_{P(1334)} + [Q_{P(1319)}/A_{(1319)}][A_{DAM} - A_{(1319)} - A_{(1334)}]$

where, Q_P : Discharge of probable flood at Dam Site

$Q_{P(1319)}$: Discharge of probable flood at No. 1319 Gauging Station

$Q_{P(1334)}$: Discharge of probable flood at No. 1334 Gauging Station

A_{DAM} : Catchment Area of Dam Site
Master Plan Dam Site $A_{DAM} = 1,994\ km^2$
Upper Dam Site $A_{DAM} = 1,959\ km^2$

$A_{(1319)}$: Catchment Area of No. 1319 Gauging Station $A_{(1319)}$ 766.4 km^2

$A_{(1334)}$: Catchment Area of No. 1334 Gauging Station $A_{(1334)}$ = 1,102 km^2

6.6 Probable Maximum Flood

6.6.1 Probable Maximum Precipitation (PMP)

Probable maximum flood (PMF) is calculated by using probable maximum precipitation (PMP) which is physically maximized up to upper limitation with hydor-meteorogical method. PMP is estimated by multiplying actual precipitation during a storm by the ratio (Maximization Factor: $\gamma_m=W_m/W_s$) of the maximum precipitable water W_m (mm) to the precipitable water during the storm W_s(mm). Depths of precipitable water between EL 0 m with 1,000 mb as bottom and various heights are expressed as a function of dew-point. Because in Turkey, vapor pressure is being observed as an alternative to dew-point, vapor pressure was converted to dew-point, and used for the PMP analysis. In the basin of the project site, vapor pressure is being measured at Bolu meteorological station (EL.742 m) and observation data at the station were utilized.

The mountain range located on the southern boundary of the project basin is considered as the topographical barrier in the analysis, and precipitable water to be used for calculation (W_s or W_m) is estimated with average elevation 1,500 m of the mountain range as the bottom and 200 mb as the top of an air column. That is, precipitable water (W_s or W_m) is expressed as below.

$$W = W_1 - W_2$$

where, W: Precipitable water (W_s or W_m)

W_1: Precipitable water of the air column with 1,000 mb at EL.0 m as the bottom and 200 mb as the top

W_2: Precipitable water of the air column with 1,000 mb at EL.0 m as the bottom and EL. 1,500 m as the top

The precipitable water during a storm (W_s) was estimated by using value of 12-hour persisting 1,000 mb dew-point obtained from

representative 12-hour persisting vapor pressure during the storm at Bolu meteorological station.

On the other hand, 12-hour persisting 1,000 mb dew-point for estimate on maximum precipitable water (W_m) was selected as described below.

i) Monthly maximum 12-hour persisting dew-points were calculated with monthly maximum 12-hour persisting vapor pressures observed at Bolu meteorological station.

ii) The above dew-points were converted to monthly maximum 12-hour persisting 1,000 mb dew-points.

iii) Maximum 12-hour persisting 1,000 mb dew-point of return period 50 years was calculated by month.

iv) As 12-hour persisting 1,000 mb dew-point used for estimate on W_m, maximum on envelope curve of iii) within 15 days of storm occurrence date was selected.

Observed storms were maximized by using W_s and W_m which were estimated with the above method. Table 6-21 shows average precipitations during storms in the basin of the project and results of maximization of the storms, and the depth-duration curve of maximized precipitation is shown in Figure 6-20. Because the storm which occurred on May 1, 1975, caused maximum daily precipitation, precipitation obtained from maximization of the storm was adopted as PMP. Process of maximization is shown in Table 6-22, with reference of Figures 6-21 to 6-23.

Since PMP was calculated with unit of a day, it was necessary for conversions to be made to 6-hour units which were used as the units for the unit hydrographs described later. The conversion to 6-hour precipitation of the 24-hour PMP was performed with multiplying the maximization factor γ_m estimated in the PMP analysis by persisting precipitation data during the storm at

Bolu meteorological station compiled in Maximum Precipitation Frequency in Turkey (1990, DSI).

Uniform precipitation loss of 2 mm/hr was assumed, and increment of effective PMP for every 6 hours was arranged in the distribution to cause the maximum discharge. The time distribution of PMP was selected as shown below.

(Unit: mm)

Duration	Increment	Loss	Increment of Effective PMP
0-6 hr	35.9	12	23.9
6-12 hr	39.0	12	27.0
12-18 hr	96.4	12	84.4
18-24 hr	13.5	12	1.5
Total	184.8	48	136.8

6.6.2 Unit Hydrograph

Unit Hydrographs of the Büyüksu-Devrek River and Mengen River were prepared by using Snyder's concept of 'Synthetic Unit Hydrograph' under the conditions described below.

Precipitation Duration: 6 hours
Precipitation Intensity: 10 mm

Figure 6-24 shows the unit hydrographs of both rivers.

6.6.3 Probable Maximum Flood

PMF hydrographs of both rivers resulting from the time distribution of effective PMP were given by multiplying discharges of the unit hydrographs shown in Figure 6-24 by the increments of effective PMP. Base flow was assumed to be 20 m^3/sec, based on average runoff at the damsite (14.39 m^3/sec). Summation of the two PMF hydrographs caused by PMP and base flow

gave PMF hydrograph at the damsite. The peak discharge of 2,485 m^3/sec was rounded, and Figure 6-25 shows the PMF hydrograph with peak discharge of 2,500 m^3/sec.

Probable maximum floods of existing and planned dams in Turkey are shown in Figure 6-26.

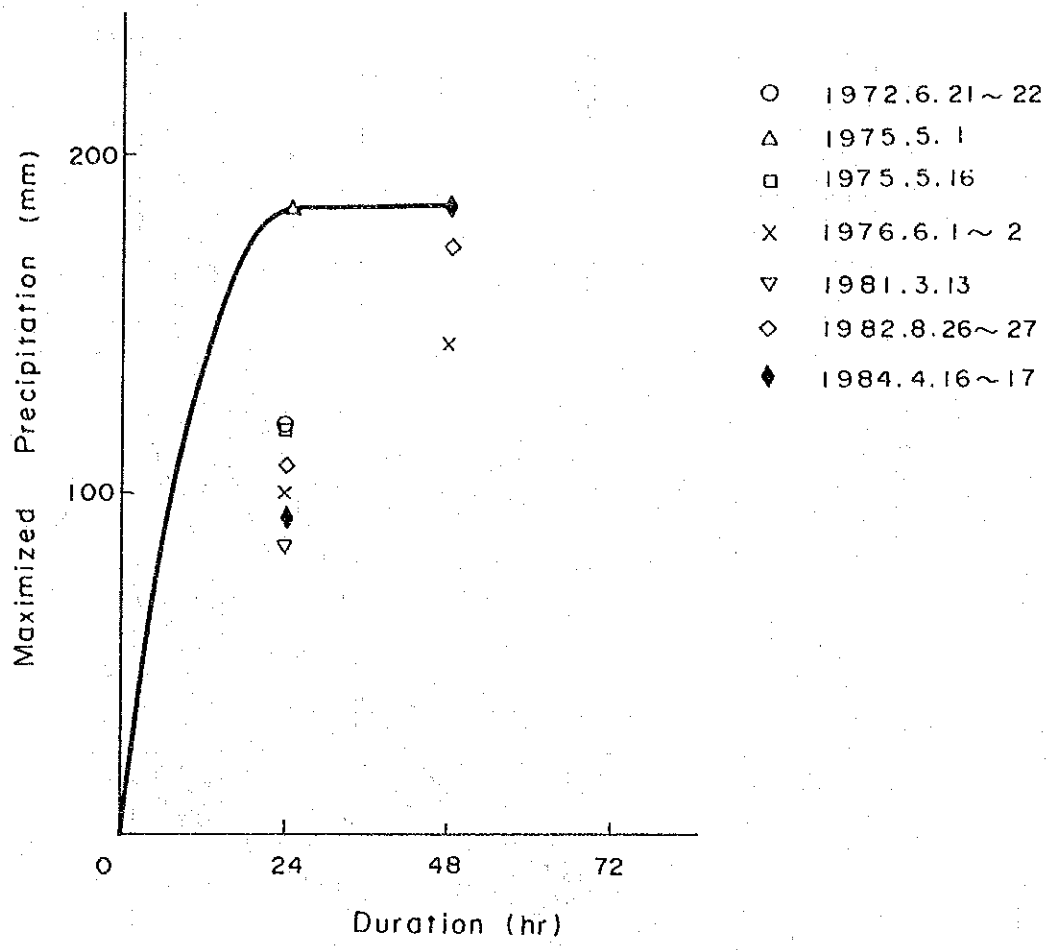

Figure 6-20 Depth-Duration Curve of Maximized Precipitation

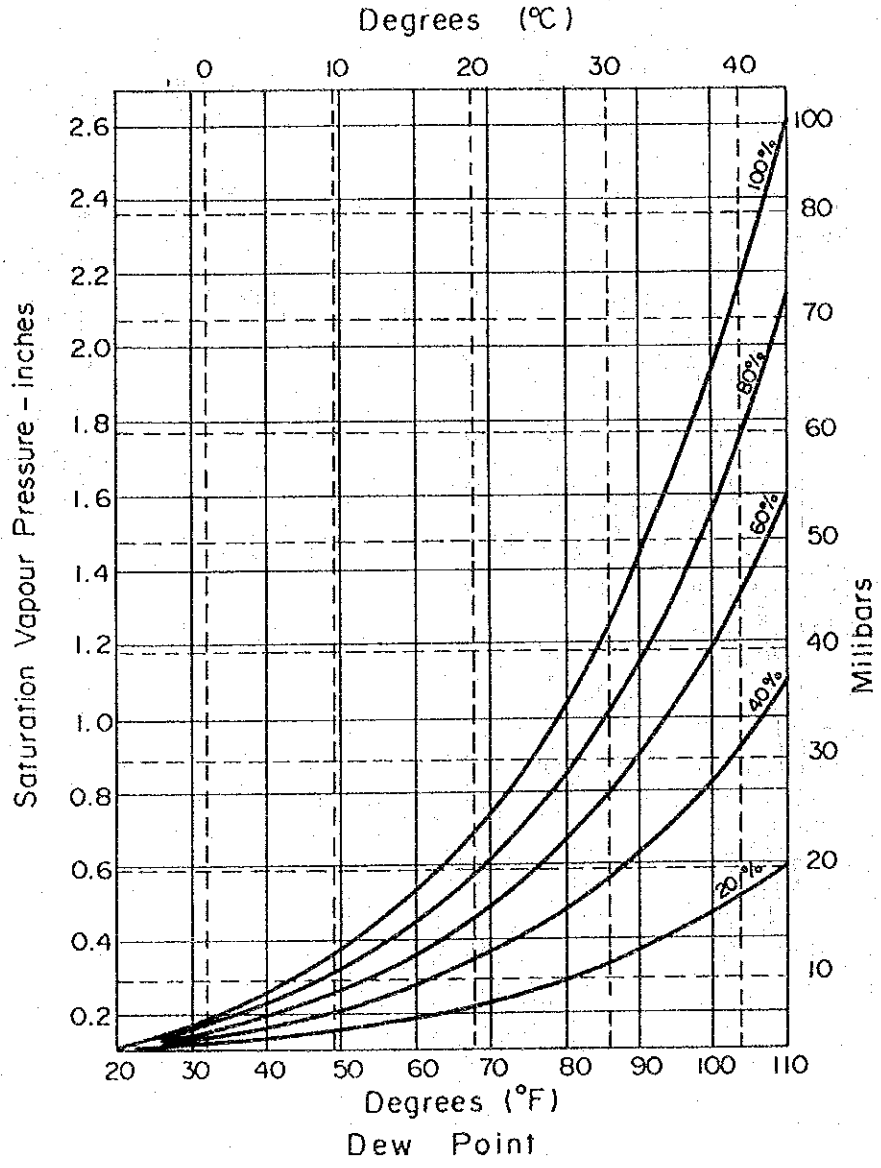

Figure 6-21 Variation of vapour pressure with temperature at percentages of saturation

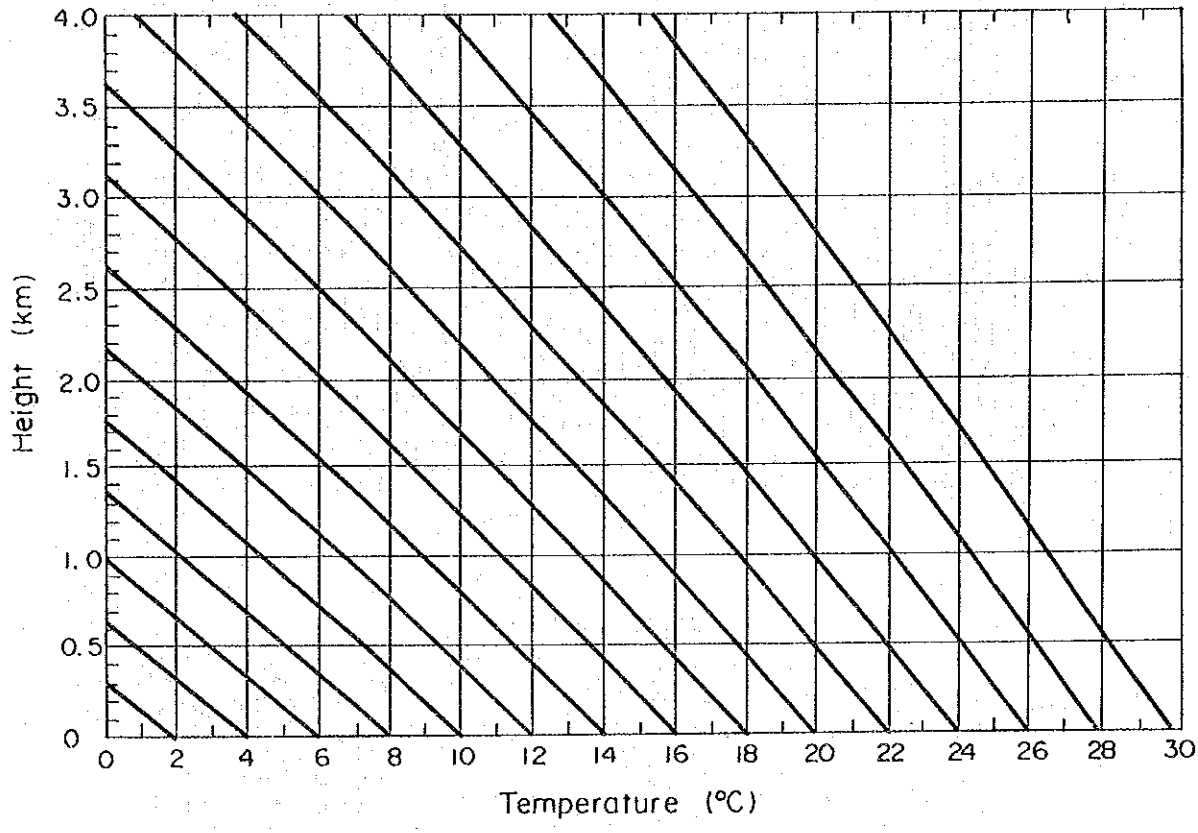

Figure 6-22 Pseudo-adiabatic diagram for dew-point reduction to 1000 mb at height zero

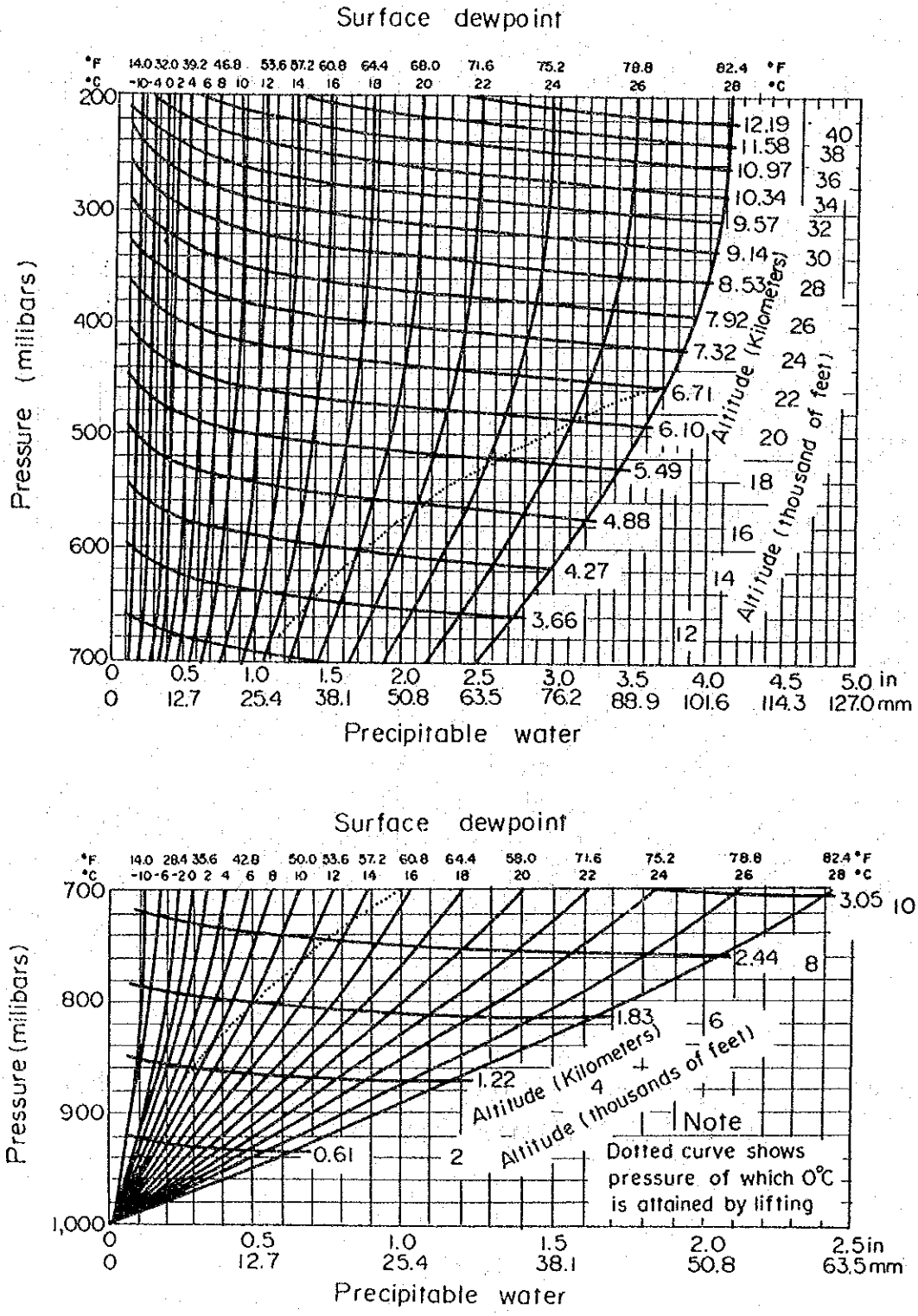

Depths of precipitable water in a column of air of any height above the 1000-milibar level as a function of the 1000-milibar dewpoint, assuming saturation and pseuda-adiabatic lapse rate. (U.S National Weather Service.)

Figure 6-23 Depths of Precipitable Water in a Column of Air

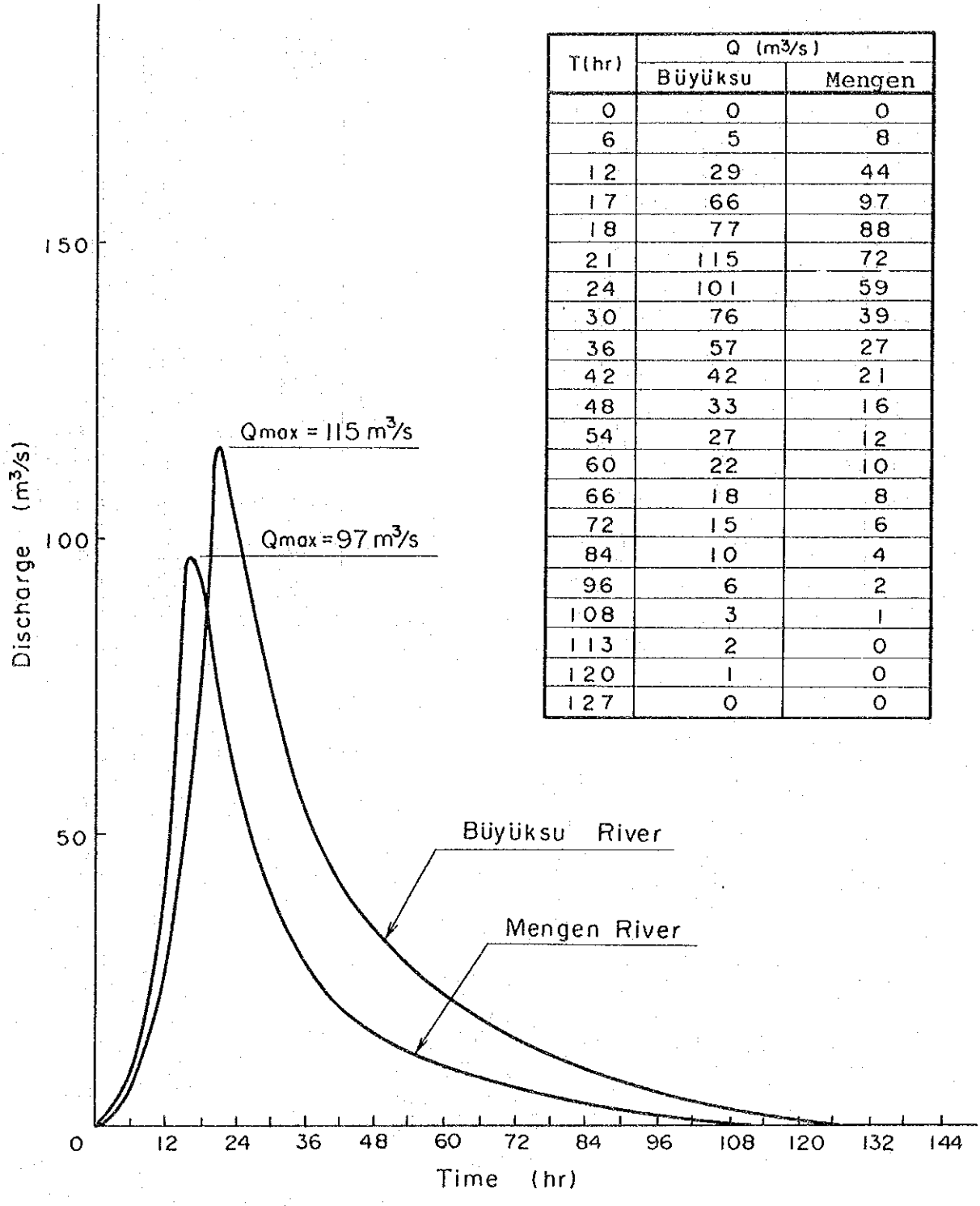

T(hr)	Q (m³/s)	
	Büyüksu	Mengen
0	0	0
6	5	8
12	29	44
17	66	97
18	77	88
21	115	72
24	101	59
30	76	39
36	57	27
42	42	21
48	33	16
54	27	12
60	22	10
66	18	8
72	15	6
84	10	4
96	6	2
108	3	1
113	2	0
120	1	0
127	0	0

Figure 6-24 Unit Hydrographs of Büyüksu-Devrek River and Mengen River

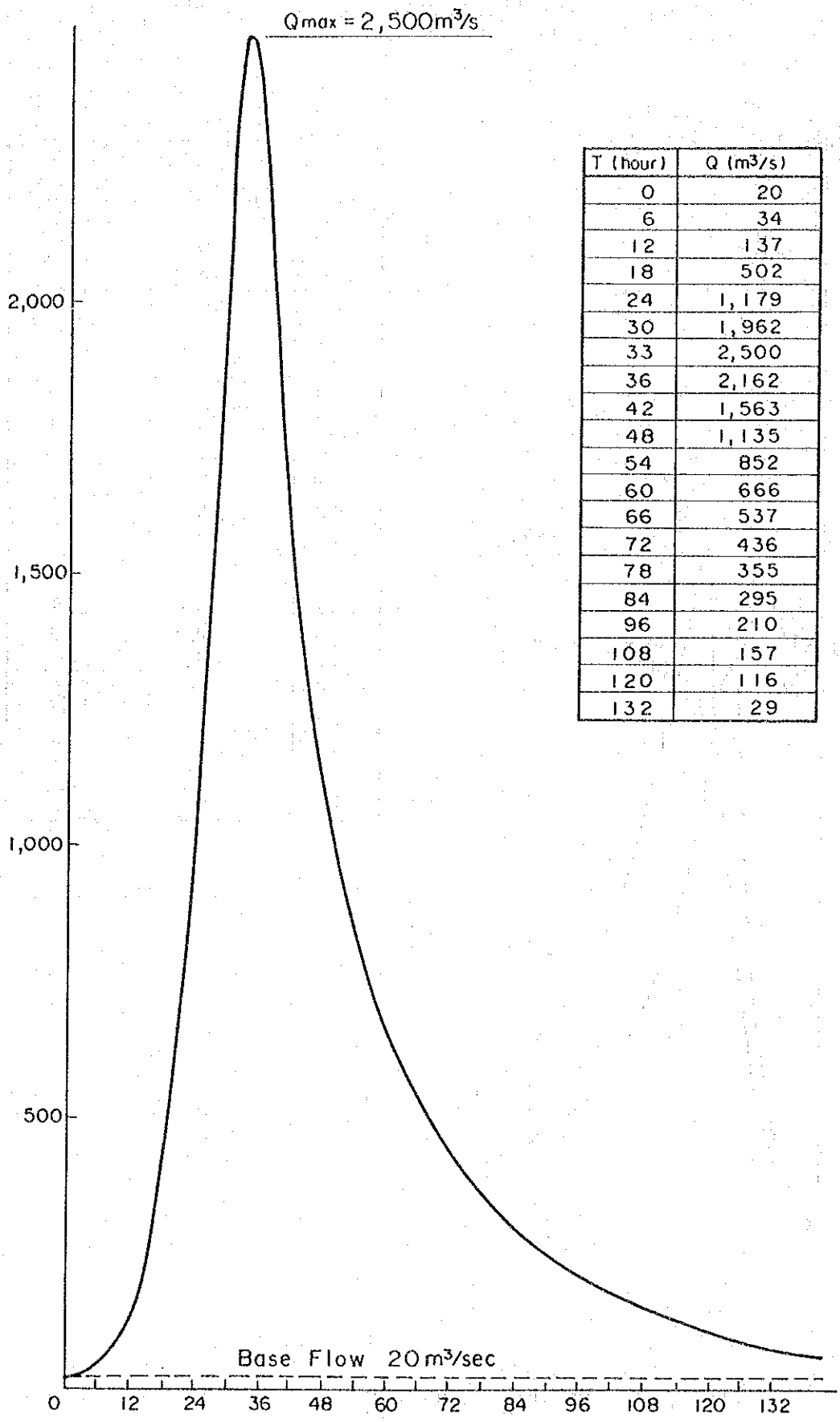

T (hour)	Q (m³/s)
0	20
6	34
12	137
18	502
24	1,179
30	1,962
33	2,500
36	2,162
42	1,563
48	1,135
54	852
60	666
66	537
72	436
78	355
84	295
96	210
108	157
120	116
132	29

Figure 6-25 Hydrograph of PMF

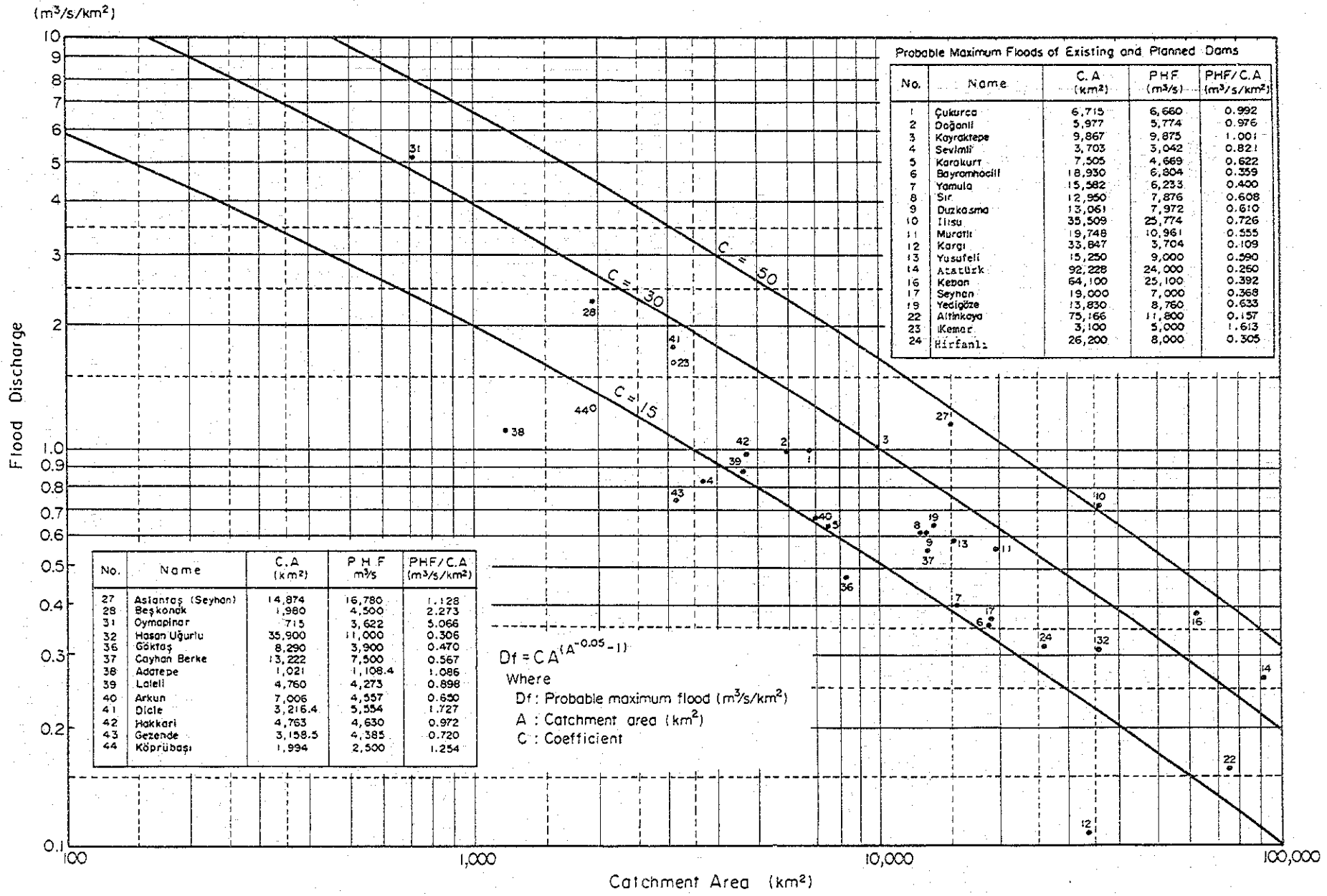

Figure 6-26 Probable Maximum Floods in Turkey

Table 6-21 Maximization of Precipitation

Storm Date (Year, Month & Day)	Storm Duration (hr)	Average Precipitation (mm)	Maximization Factor	Maximum Precipitation (mm)
1972.6.21~22	48	60.3	2.815	169.74
1975.5.1	24	42.6	4.339	184.84
1975.5.16	24	36.2	3.310	119.82
1979.6.1~2	48	53.6	2.315	124.08
1981.3.13	24	30.6	2.750	84.15
1982.8.27~28	48	75.8	2.286	173.25
1984.4.16~17	48	34.6	5.352	185.19

Table 6-22 Process of PMP Estimation during the Storm on May 1, 1975

Item	Observed or Calculated Figure
(1) Representative Dew Point observed at Bolu during the Storm (°C)	4.0°C*1
(2) Reduction of (1) to 1,000 mb at EL.0 m (°C)	8.2°C*2
(3) Precipitable Water (mm)	12.0*3 - 7.0*4 = 5.0
(4) Probable Analysis on 1,000 mb Dew-Point after conversion of Monthly Maximum Vapor Pressure at Bolu to 1,000 mb Dew-Point at EL.0 m	-
(5) Maximum 1,000 mb Dew-Point of Return Period of 50 Years at that time	16.1°C
(6) Precipitable Water (mm)	37.7*3 - 16.0*4 = 21.7
(7) Maximization Factor (6)/(3)	4.339
(8) Average Precipitation observed in the Project Area (mm)	42.6
(9) Maximization of (8) (7) x (8) (mm)	184.84

Note: *1 Vapor Pressure is converted to dew-point by using a curve of saturation of 100% in Figure 6-21
*2 See Figure 6-22
*3 Precipitable Water between 1,000 mb at EL.0 m and 200 mb (See Figure 6-23)
*4 Precipitable Water under topographic barrier of EL.1,500 m (See Figure 6-23)

Chapter 7 GEOLOGY AND CONSTRUCTION MATERIAL

Chapter 7

GEOLOGY AND CONSTRUCTION MATERIAL

Contents

List of Figures

List of Tables

Chapter 7 GEOLOGY AND CONSTRUCTION MATERIAL

7.1 Geology

7.1.1 Introduction

Regarding the layout of the principal civil structures in the electric power generation scheme of the Köprübaşı project, there have been five proposals offered including the proposal made at the stage of the Master Plan, and a comparison study was conducted based on the results of the first field investigations carried out in October 1992 by the DSİ and the JICA Survey Team and the results of analyses of existing data. As a consequence, as previously mentioned, it was decided to carry out additional investigations on A Layout (Headrace Tunnel-Open Air Powerhouse Type) and D Layout (Underground Powerhouse-Tailrace Tunnel Type) and make a comparison study of the two because they are superior to the other options. These additional investigations were started in the middle of April 1993 after waiting for snow in the investigation area to melt and were continued into October.

In this chapter, from 7.1.2 to 7.1.4, the results of organization, analyses and evaluations of data obtained regarding geology, topography, and construction material of the Köprübaşı Project through data gathering, field investigations, and geological investigation works carried out during the period from October 1992 to October 1993 by the JICA Survey Team in cooperation with the DSİ are described.

The outlines of the various investigations made at the project site for the Feasibility Study and the wide-area geology are described in 7.1.3 and the geology of the project site in 7.1.4.

The principal data related to this chapter are compiled in Table 7-1 to Table 7-7 and Figure 7-1 to Figure 7-16, and the basic data used in preparation of these figures are compiled in Appendix A-3-1 to Appendix A-3-6.

7.2.2 Outline of the Investigations

(1) Existing Data and Geological Prospectings

The existing data used as references in preparing this Report are as listed in Table 7-1.

Table 7-1 List of Existing Geological Data

No.	Title	Description	Publishing Organization
①	Geology of Köprübaşı Dam	Report and Drawings of Geological Plans and Sections	DSİ
②	Bolu-Mengen; Köprübaşı Project, 1991	Report and Drawings concerning Construction Materials	DSİ
③	Köprübaşı, Doğanözü, Peçenek Baraj Yeleri Deprem Risk Analizi, 1992	Seismic Risk Analysis Report	DSİ
④	Geological Report of Filyos-Köprübaşı Damsite, Vol. I, II & III, 1964	Report and Drawing of Geological conditions	EIE

(2) Additional Investigation Works

Various geological investigations and construction material investigations were carried out in this project area by the EIE in 1964 and the DSİ in 1992, and the results of these investigations have been compiled in the form of reports as previously mentioned at Table 7-1.

As a result of reviewing these existing reports, it was found necessary for the respective geological and engineering geological characteristics to be explained in somewhat more detail considering the project area, and principal civil structure sites in order to carry out a Feasibility Study for this Project. Therefore, geological investigations, and

geophysical explorations were planned as additional investigations, and these investigations (including in-situ tests and laboratory tests) were carried out as described below.

a) Geological Investigations

i) Aero-photo Interpretation

Aero-photo interpretations were made to obtain basic data for explaining the topographical and geological characteristics of the project area.

The scope of aero-photo interpretations considered included an area covering the powerhouse site, waterway route, damsite, reservoir area, and construction material sites, corresponding to a range approximately 15 km long in the northwest-southeast direction along the Devrek River, and approximately 8 km wide with the Devrek River roughly at the middle, the scales of the photographs used being 1/15,000 and 1/35,000. The major items of interpretation were vegetation, land use mode, geological boundary, lineament, drainage pattern, kick-point of slope, outcrop of basement rock (for example, cliff), karst topography, fan area, terrace, landslide topography, colluvial topography, surface water emergence, etc.

ii) Geological Mapping

Geological reconnaissances had already been carried out on the project area, the damsite of the Project, the reservoir area, and construction material collection sites by the EIE and the DSİ, and these had been compiled in the form of geological maps. These maps were of sufficient accuracy for preparing a master plan for the Project, but for the Project to be raised to the level of feasibility it was necessary for additional geological mapping to be done with the

purpose of evaluating the engineering geological properties of the principal civil structure sites and the reservoir area.

The sites on which additional geological mapping was done for the project area and the outlines of specifications for the investigations at these sites are as given in Table 7-2.

iii) Core Boring Investigations

In the Feasibility Study for this Project a comparison study was made of the two proposals of A Layout and D Layout for layouts of the power generation scheme structures based on the results of the various investigation data and field reconnaissances carried out. Therefore, core boring investigations (12 holes, total length 765 m) and hydrogeological investigations (drillhole water level measurements in all drillholes and lugeon tests in part of the drillholes) utilizing the drillholes are as given in Table 7-3 and Figure 7-1. Along the dam axis, there has been enough core investigation data therefore we only checked the core.

iv) Laboratory Tests

The powerhouse in the D Layout of power generation scheme structures of this Project would be an underground type and in this case it will be necessary to know the physical and mechanical properties of the surrounding rock of the underground powerhouse site.

Therefore, laboratory tests, namely, petrographic microscope examinations, density measurements, and uniaxial compression tests addition to the geological and geotechnical observation, were carried out on a boring core (DDV-1).

Additional uniaxial compression tests for 5 pieces of SK-1 and TSK-3 were carried out in order to know the general geotechnical characteristics at the dam site.

b) Geophysical Exploration

The penstock in the A Layout power generation scheme structure of this Project is planned along the comparatively rounded ridge at the right-bank side of the Devrek River, and the powerhouse at the foot of that ridge, while the tailrace is planned to pass the terraced portion formed along the right bank of the Devrek. The tailrace tunnel of D Layout is to pass under a ridge further downstream than the ridge where the penstock of A Layout will run, with the final section of the tailrace passing the same terraced portion as mentioned above. Since there are few outcrops of basement rock where these structures pass and the geological conditions are unknown, it was necessary for engineering geological properties of the surroundings of these structures or the foundation ground to be grasped. It was for this reason that the seismic exploration (diffraction method) indicated in Table 7-4 and Figure 7-1 was carried out.

Table 7-4 Seismic Prospecting (Refraction Method) Planning

Line No. (Temporary)	Location	Length	Remarks
SA-1	Surgetank site/penstock route - A Layout	800	
SA-3	Penstock route/Powerhouse site - A Layout	300	Intersecting with SA-4
SA-4	Penstock route - A Layout	150	Intersecting with SA-3
SA-5	Powerhouse site/tailrace canal route - A Layout	300	
SD-1	Tailrace tunnel route - D Layout	350	2 lines
SD-2	Tailrace tunnel route - D Layout	100	Intersecting with SD-1
SD-3	Tailrace canal route - D Layout	300	
	7 Lines:	2,300	in total length

7.1.3 Regional Geology

(1) Topography

Geographically, the territory of Turkey is partly in eastern-Europe as the east end of the Balkan Peninsula (Trakya), while the greater part is the Anatolia Peninsula (Asia Minor Peninsula) at the western end of the Asian Continent surrounded by the Black Sea and the Mediterranean Sea, the shape being rectangular as a whole fitting in a length of approximately 1,600 km east-west and width of approximately 550 km north-south.

The topography of Turkey as a whole reflects the geological structure and is featured by a structural topography of a roughly east-west nature and consists broadly of three belts: the Pontos Folded mountain system belt, the Anatolia Plateau belt to the south which makes up the backbone of the Anatolia Peninsula, and the Taurus folded mountain system belt which is still further to

the south and extends east-west along the Mediterranean Sea while accompanied locally by bending.

The Devrek River which is the object of development in this Project is a tributary of the Filyos River emptying into the Black Sea at roughly the middle of the western half of the whole of Turkey, and is one of the rivers in the Pontos folded mountain system as shown in Figure 7-3. The Büyüksu River (river length approximately 50 km) which rises from the southwest outskirts of Bolu, a major city on the arterial route connecting İstanbul and Ankara, and flows down in the southeast direction, and the Mengen River (river length approximately 50 km) which goes by Mengen, a town in the mountain land, merge in the vicinity of the small hamlet of Gökçesu, where the name changes to the Devrek River. The Devrek, downstream of the confluence, flows down in the northeast direction, at times bending sharply in the northwest direction, runs down approximately 75 km in the northeast direction on the whole to join the Yenice River (river length approximately 280 km) which becomes the above-mentioned Filyos River (river length 30 km) at the downstream most section.

The damsite of this Project is located on the Devrek River approximately 20 km downstream along the Devrek from the confluence of the Büyüksu River and the Mengen River.

The Devrek River in the project area is composed of alternating parts flowing parallel to the geological structure and parts which flow crossing the structure, and in general, the latter parts mostly consist of V-shaped valleys. Mountains with peaks from elevations of around 1,000 m to 2,000 m both sides of the Devrek River in the project area in the southwest-northeast direction on the whole, and the figures of the mountains are comparatively rounded. As for inclinations of slopes, those rising from the Devrek River are the steepest in general due to downcutting actions of the river.

Regarding large-scale landslide or colluvial areas in the project area, no unstable topographies can be recognized so far as seen

from results of field geological reconnaissances, existing topographical maps, and aerial photographs obtained for topographical and geological analyses for the Project.

On the other hand, Landsat images, as shown in Figure 7-2, clearly indicate the existence of a lineament in roughly the east-northeast to west-southwest direction passing through places such as Bolu and Gerede to the south of the project area. It is obvious that this lineament corresponds to the North Anatolian Fault, and it may be pointed out that it will be necessary hereafter to study in more detail the topography and fault activity in relation to this lineament.

(2) Geology

The territory of Turkey, from the standpoint of geological structure in general, makes up a part of the Alpine-Himalayan-Indonesian orogenic belt. Structurally, Turkey indicates an approximately east-west geological structure and may generally be divided into belts extending roughly east-west in the Anatolian land mass, namely, the Pontides belt along the Black Sea coast, the Anatorides to the south occupying the central part of the Anatolian Peninsula, and the belt along the Mediterranean Sea divided into the Taurides in the west and the Border Folds in the east. The project area is located at the west part of the Pontides out of the above-mentioned geological structure belts.

The western region of the Pontides belt, according to recent related material, may be further subdivided geologically into the Istanbul zone and the Sakarya zone. The İstanbul zone comprises a continental fringe belt (continental terrace) with a Precambrian metamorphic rock basement, and is featured by Paleozoic sedimentary rocks (Cambrian Period-Permian period) in a comparatively quiet environment. In contrast, the Sakarya zone does not include Paleozoic strata as primary strata. The Istanbul zone occupying the northwest part of the Pontides belt tectogenically overlies the Sakarya zone to the south.

According to the above division, the project area belongs to the Istanbul zone.

Regarding the geology of the project area there are already reports compiled by the EIE (1964) and another compiled by the DSİ (1987).

The opinions of the above-mentioned two agencies concerning the geological outline of the project area are the same generally speaking, but there is a difference in judgement of the geological ages with regard to strata in part. Here, the results of geological explorations carried out jointly by the DSİ and this Survey Team are described below.

As shown in Figure 7-3, various rocks belonging to Precambrian, Paleozoic (Devonian-Silurian), Mesozoic (Cretaceous), Cenozoic (Tertiary and Quaternary) times in terms of geological age are distributed in the mid-stream to upstream stretches of the Devrek River where the project area is located, and these rocks show roughly southwest-northeast directionality paralleling the North Anatolian Fault from the standpoint of geological structure.

A geological map of the project area is given in Figure 7-4 and the geologic sequence in Table 7-5.

Table 7-5 Geologic Sequence of the Project Area

Geologic Age	Lithologic Characters	Remarks
Quaternary	Alluvium: Silt, sand, gravel Terrace: Slightly cemented gravel, sand and gravel Slope Wash: Boulder, cobble, pebble, with some fine-grained materials	Reservoir Area Damsite Waterway route and powerhouse site
Upper Paleocene	Flysch: Claystone, marl, sandstone	Reservoir Area
Upper Cretaceous	Limestone	
Lower-Middle Jurassic	Granitoid: Granite, granodiorite	Damsite, waterway route, powerhouse site and reservoir area
Paleozoic-Pre-Cambrian	Metamorphic Series Green Schist; Sericite, chlorite, aktinolite schist Crystalline limestone Gneiss, amphibolite Altered Gyanodiorite	Reservoir area
Age Unknown	Porphyry	Waterway route

These rock masses of various geological ages contact each other by faults (including estimated faults) of northeast-southwest directionality or unconformity, and the Devrek River in the project area on the whole cuts across the above-mentioned rock masses.

The principal civil structures of the Project would all be provided in areas where Mesozoic (Lower-Middle Jurassic Epochs) granitic rocks are distributed, while in the reservoir area there are distributed granitic rocks of the Mesozoic (Lower-Middle Jurassic Epochs) and metamorphic rocks of Paleozoic to Precambrian and flysch of the Cenozoic (Upper Paleocene Epoch).

7.1.4 Site Geology

(1) Reservoir

a) Topography

The reservoir area, as shown in Figure 7-4, is located at the upstream part of the Devrek River, in mountainland where the river, while repeatedly showing small bends, flows in the northwest direction as a whole. The Devrek River in the area to become the reservoir forms V-shaped valleys at numerous places so that the reservoir will have many parts in contact with steep slopes. The shape of the reservoir is slender and except for two pockets formed by gullies of lengths less than 2 km at the right-bank side immediately upstream from the dam, there are no tributaries or gullies running into the reservoir to form large pockets. The length of the reservoir will be approximately 15 km along the Devrek River.

The mountain bodies surrounding the reservoir are of heights from 350 to 1,400 m, and except for the gentle slope approximately 1 km wide in the NE-SW direction at the most upstream part of the reservoir, a rugged topography is presented as a whole. There are terraced flat lands and river beds distributed along the Devrek River, but these are not of very large sizes. Development of fans is not seen either.

Judging by results of study of topographical data and of field reconnaissances, except for the old landslide topography seen at the gentle slope at the most upstream part of the reservoir area, unstable topographies of large-scale landslides and collapses are not seen. According to the results of aero-photo interpretation, there are lineaments extending several kilometers in the N-S, E-W, or NE-SW directions, but nothing was confirmed to be a distinct fractured zone in field reconnaissances.

b) Geology

In the reservoir surroundings there are Paleozoic-Precambrian metamorphic rocks, consisting of gneiss, schist, crystallins limestone, and altered granitic rocks, Mesozoic-Jurassic granitic rocks, Cenozoic-Tertiary flysch and, Quaternary deposits mainly consisting of terrace deposits, talus and river-bed deposits distributed as shown in Figure 7-4. Detailed distributions are described below.

In this report, the geological age of metamorphic rocks is Paleozoic-Precambrian according to the existing DSİ geological report (see Table 7-1) although there is the other publication which says that the age of these rocks are newer than Precambrian.

On both banks at the downstream part of the reservoir there are granitic rocks of the Mesozoic Jurassic Period distributed where the dam, waterway, and powerhouse are to be located. These granitic rocks consist of coarse-grained granodiorite and altered granodiorite, and schistose structures of strikes N-S to NW-SE and dips 50° to 70°E-NE or strikes EW to NW-SE and dips 10° to 70°S-SW are seen in parts. Diabase several tens of centimeters in width having strikes E-W to NW-SE and dips 40°-90°S to SW is locally intruded into the altered granodiorite. Predominant joints are in the three directions of N50° W60° NE, N30° E65° NW, and NS50°W.

On both banks at the midstream part of the reservoir there are distributed Paleozoic-Precambrian metamorphic rocks consisting of gneiss, schist, crystallized limestone, and altered granitic rocks. The schist contacts the previously-mentioned Mesozoic-Jurassic granitic rocks and Paleozoic-Precambrian altered granitic rocks in unconformity at the NE-SW geological boundary, and is distributed in the NE-SW direction in a width of approximately 1 km. This schist exists intermixed with

gneiss and altered granitic rocks in parts with the direction of predominant schistosity having a strike of NE-SW and dip of NW 30°-50°.

Altered granitic rocks are of three kinds: ① that distributed in the NE-SW direction with a width of approximately 2 km and contacting schist and gneiss in unconformity, ② that distributed in gneiss in block form, ③ that distributed in the NE-SW direction with a width of approximately 1 km at the left bank contacting Cenozoic-Tertiary flysch at a thrust fault of strike NE-SW and dip in the NW direction with apparent dip of 20° as the geological boundary, and contacting gneiss in unconformity at a NE-SW geological boundary. These altered granitic rocks are intermixed with schist and gneiss at parts, and some parts have coarse-grained mineral compositions. Schistose structures with strikes N-S to NE-SW and dips 30°-70° in the E to NW directions are seen locally.

Gneiss contacts altered granitic rocks on both sides at NE-SW geological boundaries and is distributed in the NE-SW direction with a width of approximately 2 km, a portion of the southeast part contacting Cenozoic-Tertiary flysch at a thrust fault of strike NE-SW and apparently dip of 20° in the NW direction. This gneiss is often intermixed with schist, altered granitic rocks, and limestone. Schistose structures of strikes N-S to NE-SW and dips 30°-70° to SE are seen at parts.

Crystallized limestone is not distributed over a wide area and is found in block form in the abovementioned gneiss, and indicate the form of olistoliths in an olistostrome.

On both banks at the upstream most part of the reservoir, flysch of the Cenozoic Tertiary Period is distributed in a width of approximately 1 km contacting Mesozoic-Cretaceous limestone in unconformity at a NE-SW geological boundary and altered granitic rocks and gneiss at a thrust fault

having a strike of NE-SW and apparently dip of 20° in the NW direction as the geological boundary. The strike and dip of this flysch are mainly NE-SW, 30°NW.

Terrace deposits are composed of gravel, sand, and silt and are located in spots at both banks. The present river-bed deposits are mainly of gravel and medium- to coarse-particle sand, and are located in large scale at only three places at the midstream to upstream part of the reservoir. Talus deposits are distributed in small scale at places below the design high water level.

Except for the thrust fault at the upstreammost part of the reservoir of strike NE-SW and apparent dip of 20° in the NW direction, there are no prominent faults in the reservoir and surroundings. According to aero-photo interpretation there are lineaments in the north-south direction, northwest-southeast direction, and northeast-southwest direction, but none is continuous in great length, and nothing has been confirmed as a fault in surface reconnaissances.

Regarding landslides, old and small-scale ones are seen at the gentle slope of the Cenozoic-Tertiary flysch distribution zone on both banks at the upstreammost part of the reservoir, but all are located at places higher up than the high-water elevation.

c) Engineering Geology

i) Watertightness

All of the Paleozoic-Precambrian metamorphic consisting of rocks gneiss, schist, and altered granitic rocks, Mesozoic-Jurassic granitic rocks, and Cenozoic-Tertiary flysch comprising the surroundings of the reservoir are unsoluble rocks. On the other hand, distribution of Paleozoic-Precambrian crystalline limestone which may

be permeable is seen in the reservoir area. This limestone indicates karst properties, but this is not distributed over a wide area, and is found as blocks surrounded by gneiss and is in the form of olistoliths in an olistostrome, so that the continuity of limestone is found to be not so distinct. Therefore, it may be considered that there will be hardly any possibility of water in the reservoir being leaked to other river basins. Topographically, there are no features such a scraggy ridges and saddles causing concern about leakage to other river basins with the exception of the ridge at the bank on the right side of the dam. On overall consideration of the above investigation results, the rugged topography around the reservoir, and the condition of water flow in gullies, it is judged that there will be no problem about water-tightness of this reservoir.

ii) Stability of Slopes

Large-scale landslides and collapses are not seen in the reservoir area or at surrounding slopes of the reservoir, and problems of stability of the reservoir rim and sudden large-quantity introduction of sediment into the reservoir are not noticed.

The old landslide topographies seen at the gentle slope around the upstreammost part of the reservoir are of small scale and located at places above the reservoir high water level. Therefore, they are judged not to be what would harm the stability of the reservoir.

Further, talus deposits distributed are of small scale, and are considered not to be detrimental to stability of the surrounding slopes of the reservoir.

(2) Dam

a) Dam Site (Master Plan Site)

i) Topography

The dam site, as shown in Figures 7-5, 7-6, and 7-7, is located where the Devrek River repeatedly makes large bands, and the dam axis is at the tip of a ridge protruding out from the right-bank side to the left-bank side (north to south) where the flow channel turns west. The high-water level of the reservoir is planned at an elevation of 437 m and the river-bed elevation in the vicinity of the dam axis is approximately 350 m. The shape of the valley at the dam site, as shown in Figure 7-7, is a U with the top opened up, and the valley widths at the high-water level and the river bed are approximately 500 m and approximately 50 m, respectively.

The ridge at the right-bank side of the dam site has a saddle (elevation approximately 450 m) part way which governs the upper limit of the reservoir. The diversion tunnel, as shown in Figures 7-5 and 7-8, is planned at approximately EL. 340 m of this right-bank ridge. The spillway, as shown in Figure 7-6 and 7-10, is also planned at the right-bank side taking advantage of the saddle, and is to be an open channel. The flip bucket portion of the spillway and the opposite bank slope indicate terrace topographies.

The dam site, except for small collapses due to minor faults and jointing immediately upstream of the left-bank abutment, indicates a stable topography at both the slopes on both banks and the right-bank side ridge.

ii) Geology

The basement rock at the dam site, as shown in Figure 7-5, comprises granitic rocks of the Mesozoic Jurassic Period and diabase intruded in them at parts. Fresh bedrock is hard and dense. These granitic rocks, according to results of microscopic examinations of thin sections of rock, consist of a granodiorite having a holocrystalline composition, but color minerals have been replaced by biotite, chlorite, epidote, sericite, etc. on being subjected to alteration. These are shown subdivided into the three levels of strong alteration, medium alteration, and weak alteration according to the degree of the alteration action in the boring and geologic profiles shown in Figures 7-6 to 7-11. Further, according to the grain sizes of the constituent minerals, those of about 4 mm and larger grain size are differentiated as coarse-grained granodiorite. The degree of alteration of coarse-grained granodiorite is comparatively small around the dam site.

The projected sites of the dam, spillway, and diversion tunnel are in the area of distribution of a dark greenish-gray granodiorite having a large amount of medium-grained to fine-grained color minerals. According to surface reconnaissances, there were schistose structures of strike E-W to NW-SE and dip 20°-60°S to SW in parts of the granodiorite subjected to alteration action. The strike and dip of this are in harmony with strongly altered zone and moderately zone estimated from boring at the dam site. Hair cracks are developed parallel to this schistose structure in the granodiorite strongly subjected to this alteration. According to the results of unconfined compression tests, the test pieces were often fractured along these hair cracks. Diabase partially intruded into the granodiorite.

The intrusion planes of diabase generally cross diagonally with the dam axis and have strikes and dips of E-W to NW-Se 50°-90°S to SW inclined toward the downstream side. The intrusions are of widths mostly from several tens of centimeters to several meters and are distributed to the same degree at both the right and left banks. Deterioration of the bedrock is not seen and both the diabase and the surrounding granitic rocks are sound.

Large-scale faults continuous over great lengths and accompanied by wide fractured zones do not exist. Only three small-scale faults of fractured widths 10 to 20 cm have been confirmed in surface explorations. Their strikes and dips are NS40°W, N35° W56°SW, and N75° W53°SW. Joints are developed in general at spacings of 10 to 40 cm, and those of strikes and dips in three directions, N50° W60° NE and N10° E45° E tending to strike to the right abutment of the dam and N60° W50° SW tending to strike to the left abutment are predominant. In boring investigations, fractured zones of section lengths not more than 2 m with mainly showing alterations of strong or medium degree have been confirmed near depths of 52 m and 65 m in SK-5, a depth of 64 m in SK-6, a depth of 28 m in SK-7, 28 m in TSK-2, 22 m and 30 m in TSK-3, 22 m and 24 m in TSK-4, and 14 m in DSK-1, but none indicating a large-scale fault accompanied by a wide fractured zone has been confirmed. In boring investigations there were many of small angles of 20° to 60° along hair cracks associated with alteration seen. This may be pointed out to be the possibility of fracturing along hair cracks during drilling.

Rock surfaces are often found to be weathered and discolored to brown near the ground surface. According to boring investigations, weathered discoloration along

fissures are prominent to depths of 10 to 30 m at the projected dam site.

As surface deposits, topsoil is distributed in thicknesses of several meters on both banks, and terrace deposits of approximately 10 m are distributed at the ground surface of the projected diversion tunnel site, with these consisting of round gravels of 10 cm diameter, sand, and silt.

The thickness of river-bed deposits, according to the results of drillholes performed at three locations, is approximately 15 m. River-bed deposits are mainly of gravels of diameters 1 to 6 cm, sand, and silt.

Talus deposits are distributed only in small scale at bases of slopes.

iii) Hydro geology

1. Groundwater Level

The final water levels in the boreholes drilled at the dam site and right-bank side ridge are shown in Figures 7-7 to -12. The groundwater level at the river-bed portion is at the same elevation as the river-bed water level of approximately 340 m. The groundwater levels at both banks of the dam site, although gently, rise in accordance with the topography, and are at approximately 7 to 26 m from the ground surface. The groundwater levels at both slopes of the right-bank side ridge, although gently, rise in accordance with the topography, and are at approximately 5 to 20 m from the ground surface. These depths are in step with the depths from the ground surface of weathering and with depths of bedrock deterioration, and there are no boreholes

which especially indicate abnormal conditions of the ground water levels. Abnormalities were not seen in groundwater levels during drilling either. The deepest groundwater level at the slope of the projected dam site was at a depth of 26 m in Drillhole SK-2 at the left bank and 19 m in Drillhole TSK-3 at the right bank. Elevations of groundwater levels at the core portion of the right-bank side ridge were approximately 438 m at DSK-1 and approximately 420 m at TSK-3.

2. Permeability

Lugeon tests using drillholes were carried out at the dam site on a total of 14 holes, 441 stages, and a length of 883 m as shown in Figures 7-7 to -12 and Appendix A-3-3. These tests were performed with the foundation rock, excluding surface layer deposits and river-bed deposits, as the object, and testing intervals were made 2 m.

The results of Lugeon tests were analyzed by the method below.

The test result Lugeon values (Lu) were the amount of injection (unit ℓ/m/min/10 kgf/cm^2) in the pressure of 10 kgf/cm^2.

Therefore, when injection pressure could not be raised to 10 kgf/cm^2 for some reason, values converted by the equation below were used.

$$Lu = \frac{10Q}{P \cdot L}$$

where, Q: injection quantity (ℓ/min)
L: length of test section (m)
P: injection pressure (kgf/cm^2)

From these results the permeability of the dam site may be summarized as follows:

• Dam, Left Abutment

The bedrock portion, except for 3 sections (Lu = 3 to 5) in the vicinity of 60 m depth in Drillhole SK-2, was of low permeability over entire lengths with Lu = 0 to 3 according to results of Lugeon tests at Drillholes SK-1 and SK-2.

• River-bed Portion

According to results of Lugeon tests at Drillholes SK-3, -7, and -8, a slightly high permeability of Lu = 3 to 5 was indicated to a depth of approximately 20 m from the surface of the basement rock, but permeability was low deeper down with Lu at 0 to 3.

• Dam, Right Abutment

According to results of Lugeon tests at Drillholes SK-4, -5, and 6, TSK-3, and DSK-1, sections indicating high permeabilities of Lu ≥ 3 to 10 were from the ground surface to around 10 to 30 m in depth. Deeper than depths of 10 to 30 m, low permeabilities of Lu = 0 to 3 were indicated at all sections.

• Spillway

In Lugeon tests on Drillholes DSK-1 and -2, permeability coefficients were determined for sections of 30 m from the ground surface, and at midheight of the slope, high permeabilities of Lu ≥ 3 to 10 were indicated to around depths of 10